FINAL

ENVIRONMENTAL STATEMENT

APPENDICES

ADDITION OF UNIT NO. 7
MYSTIC ELECTRIC GENERATING STATION
EVERETT, MASS.

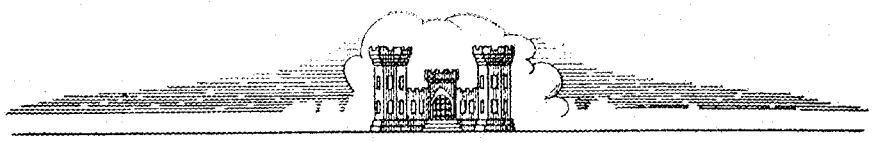

PREPARED BY

U. S. ARMY ENGINEER DIVISION, NEW ENGLAND

WALTHAM, MASSACHUSETTS

JUNE 1973

APPENDIX A

MATHEMATICAL AND TECHNICAL APPROACH

TO DIFFUSION ANALYSIS OF AIR CONTAMINANTS

APPENDIX A

MATHEMATICAL AND TECHNICAL APPROACH TO DIFFUSION ANALYSIS OF AIR CONTAMINANTS

GENERAL

The Stone & Webster dispersion model is a computer program which simultaneously evaluates station operating data and meteorological conditions to determine the hourly, daily and annual average contaminant levels for 192 fixed receptor points in the area surrounding the station. These locations lie on a 16-point compass grid and at selected radial distances extending outward from the station site.

The model incorporates the modified Gifford dispersion equation, the optimized CONCAWE plume rise equation and multiple stack effects based on work by the Tennessee Valley Authority (TVA). A detailed discussion of the dispersion model is presented later in this appendix.

Predicted annual average levels due solely to station operations are plotted on maps, and isolines are drawn to represent the spatial distribution of contaminants on an annual basis. These

levels are estimated values that could be expected if annual measurements were available from a large number of samplers and if the station were the only source in the area.

Predicted daily average levels are determined by summation of hourly concentrations occurring at fixed receptor points for a 24 hour period (12:00 A.M. to 12:00 A.M.). Maximum daily average levels are presented in bar chart form. These maximum levels are associated with persistent winds from a given direction and occur infrequently on an annual basis.

Predicted hourly levels are presented in tabular form for different operating modes and for selected meteorological conditions. The meteorological conditions are subdivided into categories with corresponding expected frequencies of occurrence which are determined by evaluating long-term climatology consisting of hourly weather data.

DIFFUSION EQUATION

Various theoretical studies on atmospheric diffusion have contributed greatly to the understanding of the physical processes involved. However, there is a trend in the analysis of gas diffusion to use a general basis that relates the diffusion characteristics to meteorological variables which are more

intimately related to the diffusion process. In these methods, statistical properties of gas concentration distributions are represented as standard deviations in place of the diffusion coefficients used by past investigators.

Pasquill[1] of the British Meteorological Office devised a method of computing dispersion from an elevated or ground-level source in terms of the height and width of the plume of airborne material, based primarily on diffusion measurements made during Project Prairie Grass (Cramer et al, 1958)[2]. Gifford[3,4] has transformed values of Pasquill's parameters of height and width to the standard deviations of plume concentration distribution in the vertical and horizontal directions. Based on the assumption that the plume has a Gaussian distribution in both the horizontal and vertical dimensions, the formula is as follows:

$$\chi = \frac{Q}{\pi \bar{u} \sigma_y \sigma_z} \exp \frac{-H^2}{2\sigma_z^2} \exp \frac{-Y^2}{2\sigma_y^2}$$

where

χ is the concentration at ground level, assuming total reflection of the plume takes place at the earth's surface

Q is the source strength (concentration at stack exit)

$\bar{u}$ is the mean wind speed affecting the plume

σ_y and σ_z are the standard deviations of plume concentration distribution in the vertical and horizontal directions, respectively

H is the height of emission

Y is the crosswind distance from the plume center line

The values of σ_y and σ_z are given in terms of downwind distance, X. The computation of concentration is, therefore, made for specific downwind distances. This formula, together with standard deviations published by Gifford[5], is the basis for Stone & Webster's computer analysis of dispersion from single stacks.

The values of both σ_y and σ_z of the dispersion equation will depend on the turbulent structure of the atmosphere. If measures of horizontal and vertical motions of the air are made (as with a bivane), the resultant records may be used to estimate σ_y and σ_z. If wind fluctuation measurements are not available, estimates of σ_y and σ_z may be made from wind measurements at the standard

height of 10 meters and estimates of net radiation, as given by Pasquill[1]. Weather stability categories (A through F) are given in Table A-1 in terms of insolation during daytime (radiation received from the sun) and amount of cloud cover at night:

TABLE A-1

WEATHER STABILITY CATEGORIES

Surface Wind Speed		Insolation			Night	
M Per Sec	Mph	Strong	Moderate	Slight	>4/8 Low Cloud	<3/8 Cloud
<2	<4.5	A	A	B	-	-
2-3	4.5 - 6.7	A-B	B	C	E	F
3-5	6.7 - 11.2	B	B-C	C	D	E
5-6	11.2 - 13.4	C	C-D	D	D	D
>6	>13.4	C	D	D	D	D

Strong insolation corresponds to a solar altitude (above the horizon) greater than 60 degrees with clear skies; it may occur on a sunny midday in midsummer. Slight insolation corresponds to a solar altitude from 15 to 35 degrees with clear skies; it may occur on a sunny midday in midwinter. However, cloudiness will

generally decrease insolation and should be considered along with solar altitude in determining insolation. Insolation that would be strong with clear skies might become moderate with broken middle clouds and slight with broken low clouds. Night refers to the period from 1 hour before sunset to 1 hour after sunrise. The neutral category D should be assumed for overcast conditions during day or night.

METEOROLOGICAL CONDITIONS

Gas diffusion rates depend upon atmospheric turbulence, which is divided into two types, convective and mechanical. Mechanical turbulence arises from movement of air over the earth's surface and is influenced by nonthermal features of buildings and any objects which resist air motion. Mechanical turbulence increases with irregularity of the surface, and its intensity increases with wind speed. Convective turbulence is caused largely by differences in temperature between the land surface and the overlying air stream. The range of temperature gradients may be divided into unstable, neutral and stable. The neutral case will show primarily mechanical turbulence, while the unstable adds convective turbulence, and the stable suppresses mechanical turbulence.

While certain thermal conditions produce convective turbulence, there are others which, instead of producing turbulence, may suppress mechanical turbulence. Thermal and mechanical influences generally occur simultaneously in varying ratios. Convective turbulence tends to have longer period fluctuations, but the two cannot be completely separated.

Pasquill's six atmospheric stability classes (A to F)[1] are related to turbulence, and each class is associated with a plume of certain geometrical form and gas concentration distribution. A looping plume occurs with a high degree of turbulence, especially convective, and is typical of a daytime condition with intense solar heating of the earth's surface causing unstable thermal conditions. (Stability Class A represents these conditions at low wind speed and extreme instability.) Rapid diffusion occurs and maximum ground level concentration may occur within one to five stack heights. Highest peak concentrations will occur momentarily with this condition. As wind speed increases and/or solar radiation decreases, Stability Class B occurs. Peak concentrations are lower than with Class A and maximum ground level concentrations may occur three to eight stack heights away. Reduced solar radiation and/or increased wind speed creates a coning plume, approximately represented by Class C, when thermal conditions are more nearly neutral and

mechanical turbulence is predominant with maximum ground level concentrations occurring 10 to 13 stack heights away.

As solar radiation becomes insignificant (because of cloud cover and/or darkness) and wind speed intensifies, the coning plume begins to change to a fanning plume. This condition is caused primarily by isothermal conditions, and vertical diffusion becomes less rapid than that of Class C. Class D stability can occur during both day and night at any time during the year. Classes E and F represent progressively more stable conditions at night, with Class F occurring at lower wind speeds than Class E. Mechanical turbulence is suppressed and very little vertical diffusion occurs. Therefore, maximum ground level concentrations may occur more than 50 stack heights away. A fanning plume is likely to occur under these stable conditions, and the plume will remain intact for a considerable downwind distance. Pasquill does not classify the very stable condition which may occur at even lower wind speeds than those of Class E or F. The vertical diffusion is minimal and cannot be detected at great distances downwind.

Weather stability classes and related conditions are presented in Table A-2.

PLUME RISE EQUATION

Many procedures have been developed for use in estimating the rise of gas plumes. Some are entirely empirical in development; others are based on theoretical analyses with subsequent modifications resulting from experimental information. Over the past 15 years, the improved capability for estimating plume rise has brought about a more accurate and confident assessment of diffusion problems.

Table A-2

Dispersion Phenomena Associated Meteorological Conditions

Stability Class	Stability Condition	Plume Description	Type of Turbulence	Relative Wind Speeds, Knots	Time of Day	Season
A	Very unstable	Looping	Largely thermal	1-5	1000-1500 only	Uncommon in winter
B	Moderately unstable	Looping	Largely thermal	1-9	0900-1500	Mostly summer
C	Slightly unstable or near neutral	Coning	Mostly mechanical	1-11	0600-1700	Any
D	Neutral	Fanning	Mechanical	Any	Night or day with/ without heavy cloud cover	Any
E	Slightly stable	Fanning	Mechanical	4-10	Night	Any
F	Moderately stable	Fanning	Negligible	1-6	Night	Any
G	Extremely stable	Fanning	Negligible	1-3	Night	Any

In 1963, the Tennessee Valley Authority, under the sponsorship of the Public Health Service, initiated a plume rise study at six of its electric generating stations. The purpose of this study was to determine and compile plume rise observations from these plants under a wide variety of operational and meteorological conditions. These observations were later correlated with postulated plume rise formulas to determine the most appropriate equation to be used for a generalized dispersion study. The results of this study are contained in a 1968 TVA publication entitled "Full Scale Study of Plume Rise at Large Electric Generating Stations"[6] and in a recent publication entitled "Plume Rise Estimates for Electric Generating Stations."[7]

From the plume rise study, TVA concluded that several formulas can be used effectively to estimate the rise of gas plumes. These formulas were optimized by regression analyses to best fit TVA data. The CONCAWE and the Csanady equations, as well as the "2/3 Power Law" relation, were selected as the three best equations. The CONCAWE equation was considered preferable for most general investigations since it correlates well with both TVA and European plume rise observations; the optimized CONCAWE equation was used in this report and is as follows:

$$\Delta h = 0.414 \frac{Q_h^{0.444}}{\bar{u}^{0.694}}$$

where:

Δh (meters) = rise at the plume center line above the stack

Q_h (calories per second) = heat emission from stack

$\bar{u}$ (meters per second) = mean horizontal wind speed

When the stack gas exit velocity is lower than the wind speed, due to either low load or high wind speed conditions, the stack gases do not rise but extend approximately horizontally from the stack top. When the stack gas exit velocity is less than 1.5 times the wind speed, our analysis – based on the work of Sherlock and Stalker[8] – sets the plume rise equal to zero.

MULTIPLE STACK EFFECTS

Strom[9] states that when two or more stacks are closely grouped, they have mutual influences and their plumes tend to merge into one. Limits on this effect are given in a paper by Bosanquet et al[10] – in which it is stated that plumes from multiple stacks will rise higher than a plume from only one of them, but not as high as a plume from one stack replacing all of them.

Gartrell, Thomas, and Carpenter[11] summarize TVA's work on multiple stacks as follows:

Extensive data has confirmed that an increase in the station size as based on the number of generating units does not result in a linear or proportional increase in the maximum ground level concentrations of SO_2.

The results of their work are summarized in Table A-3. tabulation:

Table A-3

Relative Contribution to Ground Level Concentrations as a Function of Number of Units

Units on Line	Maximum Average Relative Concentration
1	1.0
2	1.8
3	2.6
4	3.3
5	3.9
6	4.4
7	4.8
8	5.0
9	5.1
10	5.3

The apparent nonlinearity in the above tabulation is due partly to greater effective plume rise and partly to the effect of a line source. When the wind blows along the line of stacks, the merging of the plumes (with less resulting heat loss) predominates, thereby increasing the effective plume rise and lowering associated ground level consideration. With the wind blowing perpendicularly to the line of stacks, the situation resembles that of a line source. The greater quantity of ambient air which is initially entrained in this case results in lower ground level concentrations downwind. The TVA study showed that the net effect on ground level concentrations from the two separate effects is more or less independent of wind direction.

RELIABILITY OF THE MODEL

To determine the reliability of the Stone & Webster dispersion model, predicted and measured average sulfur dioxide levels were compared for two Boston Edison Company monitors in proximity to the Mystic Station. One monitor, Station 3, is located 1.8 miles east-southeast of the station in East Boston; the other, Station 4, is located 1.7 miles west-southwest of the station in Somerville.

The predicted and measured average sulfur dioxide levels used in the comparison were for June, July, August, 1968, with winds blowing from the Mystic Station toward the monitors. This time period was selected to minimize effects of space heating; however, there are other industrial sources in the Mystic Station wind sector which affect the monitors during summer months. The Mystic Station was burning a fuel oil with an average sulfur content of 2.5 percent during this period.

The average sulfur dioxide levels measured at each monitor for this summer period, with winds blowing from the station to the monitors, were 0.058 ppm for Station 3 and 0.045 ppm for Station 4. The predicted levels for the same time period were 0.037 ppm for Station 3 and 0.052 ppm for Station 4. These predicted values are within acceptable ranges of the observed values.

REFERENCES

1. F. Pasquill, Atmospheric Diffusion, D. Van Nostrand Company, Ltd., 1962.

2. H. E. Cramer, F. A. Record, and H. C. Vaughan, 1958, "The Study of the Diffusion of Gases on Aerosols in the Lower Atmosphere," M.I.T. Department of Meteorology, Final Report under Contract No. AF 19(604)-1058.

3. F. A. Gifford, "Atmospheric Dispersion Calculations Using Generalized Gaussian Plume Model," Nuclear Safety, 2:56-59, December 1960.

4. F. A. Gifford, "Use of Routine Meteorological Observations for Estimating Atmospheric Dispersion," Nuclear Safety, 2:47-51, 1961.

5. F. A. Gifford, "The Problem of Forecasting Dispersion in the Lower Atmosphere," Weather Bureau Research Station, Oak Ridge, Tennessee, 1961.

6. TVA Publication, "Full Scale Study of Plume Rise at Large Electric Generating Stations," 1968.

7. F. W. Thomas, S. B. Carpenter, W. C. Colbaugh, "Plume Rise Estimates for Electric Generating Stations," APCA Journal, Vol. 20, No. 3, 1970.

8. R. H. Sherlock and E. A. Stalker, "Study of Flow Phenomena in the Wake of Smoke Stacks," Michigan University, Engineering Research Bulletin No. 29, 1941.

9. G. H. Strom, "Atmospheric Dispersion of Stack Effluents," Air Pollution, Vol. 1, ed. A. C. Stern, Academic Press, 1962.

10. C. H. Bosanquet, W. F. Carey, and E. M. Halton, Procedures of the Institute of Mechanical Engineers, 162, 335, 1950.

11. F. E. Gartrell, F. W. Thomas, and S. B. Carpenter, Journal of the Air Pollution Association, 11, 60, 1961.

APPENDIX B

ECOLOGICAL FIELD SURVEY, MYSTIC RIVER

(See Section 3.2.3.1.5 for description of additional ecological field surveys taken in June and August 1972)

APPENDIX B

MARINE ENVIRONMENTAL SERVICES

ECOLOGICAL FIELD SURVEY
MYSTIC RIVER

(1 October 1970)

Report prepared for:

Stone & Webster Engineering Corporation
225 Franklin Street
Boston, Massachusetts

Report prepared by:

N. Corwin
R. L. Haedrich
C. B. Officer
G. T. Rowe
J. H. Ryther
R. F. Vaccaro

Nugget Arcade Bldg., P.O. 679, Hanover, N. H.

TABLE OF CONTENTS

LIST OF TABLES

LIST OF CHARTS

4. Chemical Methods:

Ammonia-nitrogen

Solorzano, Lucia. 1969. Determination of ammonia waters by the phenolphypochlorite method. Limnol. Oceanog., 14: 799–801.

Nitrate and Nitrate-nitrogen

Wood, E. D., F. A. J. Armstrong, and F. A. Richards. 1967. Determination of nitrate in seawater by cadmium-copper reduction to nitrate. J. Mar. Bio. Assn. U. K., 47: 23–31.

Phosphate-phosphorus

Murphy, J. and J. P. Riley. 1962. A modified single solution method for the determination of phosphate in natural waters. Anal. Chim. Acta, 26: 31–36.

Particulate phosphorus

N. Corwin, Woods Hole Oceanographic Institution. (Unpublished method)

Total phosphorus

Menzel, D. W. and N. Corwin. 1965. The measurement of total phosphorus in seawater based on the liberation of organically bound fractions by persulfate oxidation. Limnol. Oceanog., 10: 280–282.

5. Bacteriological samples were collected with a syringe attached to and activated by the Nansen bottle, collecting discrete samples from the surface and bottom of each station. Samples were collected in sterile tubes attached to the syringe and were transferred in the field to sterile test tubes and stored chilled until returned to the laboratory. Total coliform bacteria were determined by the Millipore Filter Corp. technique, using equipment supplied by that organization, which depends upon the appearance of distinctive colonies on ENDO medium after 24 hours incubation at 37 C.

6. Benthic Invertebrates: Two bottom samples were taken with an Emery-type 1/25 m^2 bottom grab at each of five stations across each of the five transects, a total of 25 stations and 50 samples. These were sieved through 1 mm mesh screen, preserved in 10 percent buffered formalin, and returned to

the laboratory for enumeration, identification, and weighing of the organisms.

Two short sediment cores were taken from each transect, a total of 10 cores, with a Pfleger-type gravity corer. These have been stored frozen for examination of sediment type and/or the smaller, interstitial flora and fauna if comparative information of such a type appears desirable at a future date. Type specimens of the dominant invertebrates are also being stored for future reference, if and when necessary.

7. Fishes: Five bottom trawls were made with a small otter trawl (10 feet wide at mouth). Mesh was knotted, 1 inch stretched. Four trawls, each covering approximately 100 yards of bottom, were made at transects 2-5 parallel to the shore on the north side of the dredged channel, where bottom grabs had indicated a suitable bottom. An additional short bottom trawl was made in the immediate vicinity of the discharge canal of the Boston Edison plant. The bottom on the south side of the channel and in the entire upstream area of Section 1 was so soft that the trawl dug in and could not be used.

One long midwater trawl at a depth of approximately 20 feet was made along the center of the channel between Sections 2

II - SURVEY RESULTS

1. WATER QUALITY

The area between Amelia Earhart Dam and Mystic River Bridge is relatively well mixed and homogeneous. The water is weakly stratified vertically, as both temperature and salinity indicate, and the upstream part of the study area, nearest the dam, is slightly more brackish, reflecting the small input of fresh water that enters the system when the locks are opened. A tidal excursion of about six feet occurs as a wedge of colder, more saline water penetrates the region at greater depths during high tide. This tidal exchange, and the mixing of the deeper water with that overlying it, results in a very slight gradient in properties from surface to bottom. Without this tidal action the deeper waters would certainly become anoxic and devoid of life.

The level of dissolved oxygen throughout the region is low, averaging less than 50 percent of saturation at the upstream end of the system and less than 75 percent of saturation downstream. As would be expected, the oxygen concentrations are lower in the deeper water, but even at the surface, they are hardly more than 50 percent of saturation. The pH of both the surface and deeper water is also surprisingly acidic, ranging from 6.5 to 7.4 (with

one aberrant value of 3.3) at all depths, in contrast to values of 8.0 or higher for normal seawater of the salinity which occurred in the region. The low oxygen and pH levels suggest that little or no photosynthesis or organic production was taking place in the region. In other words, any aquatic life would depend upon organic matter brought into the system by tidal exchange or some other mechanism, the region being one of net consumption rather than production of organic matter.

The concentrations of inorganic nutrient chemicals (ammonia, nitrate, nitrite, phosphate) are extremely high at all depths, an order of magnitude or more greater than coastal waters in general. Particularly noteworthy are the high levels of ammonium-nitrogen, which again reach maxima at the upstream stations. High nutrient levels, and high levels of ammonia, in particular, are strongly indicative of organic pollution, and the distribution of these properties clearly show that the pollution enters the system through the locks and from the upper Mystic River.

Our research vessel was maintained at a marina in the upper portion of the Mystic River above the Amelia Earhart Dam (i.e., in freshwater). Although no studies were made on that part of the river, visual observation showed it to be characterized by a dense bloom of floating, blue-green algae as is typical of

polluted freshwater. Below the dam, there was no evidence of similar algal growth and, as mentioned above, the low values of oxygen and pH indicated the absence of photosynthetic activity, despite abnormally high levels of inorganic plant nutrients. This conflicting evidence strongly suggests that some other factor, most probably the presence of toxic chemical substance from one or more of the industries located on the banks of the Mystic River, inhibited photosynthesis and the growth of planktonic algae in the lower Mystic River.

The turbidity of the water ranged from Secchi disc readings of 5–8 feet, corresponding to a depth of photosynthesis of 18 to 25 feet. As water depths in the main channel averaged over 40 feet at high tide, it is not surprising that benthic plants were not observed in the region.

Most of the physical and chemical characteristics of the water were irregular in their distribution, suggesting that the water was rather well mixed, but also influenced by local inputs from various sources. This is also true of the distribution of coliform bacteria, which ranged from 100 to 60,000 organisms per 100 ml of water. Generally, higher concentrations of the bacteria occurred in the surface waters, as would be expected, but no distinctive pattern of upstream-downstream distribution could be detected.

With the exception of the aberrant observations at Station 1, Section 1, at high tide (pH of 3.3 and other peculiarities), the median coliform count was 10,000 cells/100 ml at the surface and 3,000 cells/100 ml in the deep water. To attach some public health significance to these figures and to give them some relative meaning, it may be of interest to compare them with prevailing U.S. Public Health Service and Massachusetts water quality standards. For bathing purposes, these are placed at coliform concentrations that do not exceed 1,000 organisms per 100 ml. For the taking of edible shellfish, three categories are recognized in Massachusetts:

Acceptable	0-70 coliforms/100 ml
Restricted (shellfish purification required)	70-700 coliforms/100 ml
Closed	Over 700 coliforms/100 ml

By these standards, the entire Mystic River within the study area would be closed to shellfishing and to bathing and would be considered heavily polluted with domestic wastes.

2. SEDIMENTS

The sediment in the entire area surveyed consisted of black silt that was anoxic a few mm beneath its surface and contained hydrogen sulfide. The single exception to this condition occurred in the area immediately adjacent to the discharge canal from Boston Edison where the water movement presumably prevented the accumulation of silt and the bottom consisted of coarse sand, pebbles, and cobble-sized rock. Beginning at Section 2, a thin layer of brown flocculent material covered the black silt. This gradually increased to a maximum thickness of about 2 mm at the farthest downstream section (Section 5). With the exception of the scoured area near the power plant, the sediment was characterized by the smell, texture, and general appearance of oil.

3. BENTHIC INVERTEBRATES

A large fraction of the upstream samples were devoid of macrobenthic life due to the anoxic condition of the sediment. The abundance of benthic invertebrates, both in terms of numbers of individuals, numbers of species, and total biomass was relatively low throughout the basin in comparison with other coastal waters of the same depth. The diversity of species was low, but tended to increase in the downstream direction. The

dominant species was polychaete worms, most commonly of the genus Capitella. The exception to this was again in the immediate vicinity of the Boston Edison discharge canal where there occurred the greatest biomass and greatest number of species, a community dominated by a large population of the edible mussel, Mytilus edulis.

Several large crabs and two sponges were taken with the otter trawl between Sections 2 and 5. There is no reason to assume that these animals did not occupy much of the lower part of the study area, where they could presumably feed upon the abundant polychaetes, but it is unlikely that they would live upstream in the region of anoxic mud where few, if any, smaller invertebrates occurred.

4. FISHES

No trawls could be taken at Section I. No fish were taken by the otter trawl at Section II or in the short trawl made in the vicinity of the discharge canal of the Boston Edison plant.

Winter flounder (Pseudopleuronectes americanus) were taken at Section III (four fish), Section IV (10 fish), and Section V (four fish). Sizes ranged from 59 mm to 280 mm, weights from 5 to 436 grams. All these fish were fat and in good condition.

Many were females with well-developed ovaries, in which the eggs for the late winter spawning were just beginning to form. Only three stomachs were empty. The most common food item was the well-digested remains of small polychaete worms of the genus Capitella. Also found was a filamentous alga, occasional hydroids, some tiny mussels, and much mud and detritus. Not uncommon in the stomachs of fish from Sections III and IV were numerous small uniform-sized particles of black soot that probably had been ingested by worms that, in turn, had been eaten by the fish.

A 160 mm fish from Section III contained two shrimps. Possibly, these were taken outside the Mystic River, as they were not otherwise seen. Fish from Sections III and IV were most similar in their feeding, with worms and mud predominating in their stomachs. Fish from Section V contained more algae, only a few worms, some sea squirts, and no mud. Examination of the scales of the smallest flounder taken showed them to be young-of-the-year. The estuary may therefore be a nursery area for this species.

Two ocean pout (Macrozoarces americanus) were taken at Section V. Although small (lengths 235 and 275 mm, weights 73 and 113 grams), both were ripe, three-year-old females that would have spawned within the month. The stomachs of both were empty.

Ocean pout are strongly territorial fish. In particular, the female guards the eggs for the three months or so required for them to hatch. The two ocean pouts taken at Section V would, in all likelihood, have spawned there, and hence young ocean pouts should be expected at some time of the year in the lower Mystic River basin.

No fishes or fish larvae were taken from the baited bottom trap, the long, mid-channel, mid-water net haul between Sections II and IV, or the oblique net hauls. The lock tender at the Amelia Earhart Dam reported a large upstream spawning migration of alewives (Alosa pseudoharengus) in the spring and large numbers of small, young-of-the-year alewives returning downstream through the locks in midsummer. He also reported that schools of mackerel (Scomber scombrus) appeared in the locks in late August. It is unlikely that there are resident populations of either species in the Mystic River basin.

Eel, presumably Anguilla rostrata, were reputed by employees of the Boston Edison plant to have been taken by hook-and-line fishing near the discharge canal, and the lock tender of the dam reported a large upstream migration of this species in August.

Table B-1

Environmental Water Quality Data - Part 1

	Water Depth, Feet	Secchi Disc, Feet	Depth, Feet	Temp., C	Salinity (0/00)	pH	O, ppm	O Sat., %
Section I	-	5	0	16.2	29.9	7.0	4.1	54
Station 1			3	16.5	30.9		2.6	35
(low tide)			6	15.8	31.4		2.5	33
			9	15.2	31.5	6.8	2.3	29
Section I	24	6	0	15.0	29.5	3.3	4.3	54
Station 1			3	15.5	33.0		3.7	46
(high tide)			6	15.8	33.0		2.7	35
			9	15.7	33.3		3.3	44
			12	15.5	33.5		3.1	40
			18	15.7	33.5		3.2	42
			24	15.4	33.5	6.5	1.8	23
Section I	-	7	0	15.9	29.6	6.9	4.5	57
Station 2			3	15.7	31.3		3.2	41
(low tide)			6	15.6	32.1		2.9	37
			9	15.6	32.1	6.9	2.3	28
Section I	20	5	0	16.0	29.8	6.5	4.5	57
Station 2			6	16.0	34.8		3.2	43
(high tide)			12	15.9	35.2		2.9	39
			18	15.9	35.4	6.9	2.3	29
Section II	32	8	0	16.7	30.8	7.2	4.9	64
Station 1			3	16.0	30.8		4.3	56
(low tide)			6	15.8	31.0		4.4	56
			9	15.6	30.9		4.2	53
			12	15.5	30.9		4.3	55
			15	15.4	31.0		4.6	59
			18	15.1	31.0	7.3	4.7	61
Section II	37	7	0	16.2	30.4	6.7	4.9	63
Station 1			6	16.2	31.8		5.3	69
(high tide)			12	16.0	31.9		5.4	69
			18	15.4	32.1		5.2	66
			24	15.1	32.2		5.1	64
			30	14.9	32.3		5.6	70
			36	14.5	32.3	7.0	5.7	72

Table B-1 (Cont'd)

	Water Depth, Feet	Secchi Disc, Feet	Depth, Feet	Temp., C	Salinity (0/00)	pH	O, ppm	O Sat., %
Section II	34	7	0	15.9	30.6	6.8	4.5	57
Station 2			3	16.0	30.7		4.4	55
(low tide)			6	16.0	30.8		4.7	61
			9	15.9	31.0		4.9	62
			12	15.7	31.0		5.0	64
			15	15.6	31.1		5.0	64
			18	15.2	31.2	7.1	4.7	61
Section II	20	6	0	16.0	29.6	6.7	3.4	43
Station 3			3	16.1	29.7		3.4	43
(low tide)			6	15.9	30.5		3.4	43
			9	15.7	31.2	6.7	4.6	59
Section II	30	6	0	16.4	30.6	7.1	4.8	62
Station 3			6	16.1	31.0		6.1	79
(High tide)			12	15.9	31.0		6.0	79
			18	15.6	31.0		5.2	66
			24	15.0	31.3		5.6	70
			30	14.8	31.5	7.1	5.6	70
Section III	40	6	0	16.0	30.1	6.7	3.6	46
Station 1			3	16.0	30.1		4.1	52
(low tide)			6	16.0	30.8		5.3	68
			9	15.8	31.0		5.3	68
			12	15.5	31.2		5.4	70
			18	15.5	31.1		5.3	68
			21	15.0	31.4	7.0	5.3	68
Section III	44	8	0	16.2	30.7	6.9	5.0	65
Station 1			6	16.2	31.0		5.2	67
(high tide)			12	15.9	31.1		5.1	65
			18	15.7	31.2		4.8	62
			24	15.2	31.5		4.7	61
			30	14.8	31.6		4.6	59
			36	14.7	31.8		4.8	61
			42	14.6	31.8	7.0	4.6	58
Section III	40	6	0	15.8	30.6	6.9	4.9	62
Station 2			3	15.9	30.6		4.5	57
(low tide)			6	15.9	30.7		4.4	55
			9	15.9	30.7		4.3	55
			12	15.8	30.9		4.5	57
			15	15.7	31.0		4.5	57
			18	15.6	31.0		4.4	55
			21	15.0	31.2	7.0	4.4	55

Table B-1 (Cont'd)

	Water Depth, Feet	Secchi Disc, Feet	Depth, Feet	Temp., C	Salinity (0/00)	pH	O, ppm	O Sat., %
Section III Station 2 (high tide)	44	8	0	16.2	30.7	7.0	5.2	67
			6	16.1	30.6		4.9	64
			12	16.1	30.8		4.9	64
			18	15.5	31.0		4.7	61
			24	14.9	31.3		4.5	56
			30	14.8	31.3		4.8	61
			36	14.7	31.4		4.5	56
			42	14.5	31.4	7.0	4.4	55
Section IV Station 1 (low tide)	46	6	0	15.4	30.9	7.0	5.3	68
			3	15.2	31.0		5.1	64
			6	15.1	31.0		4.9	63
			9	15.0	31.0		4.9	63
			12	14.9	31.0		5.0	64
			15	14.8	31.1		4.9	63
			18	14.8	31.2		4.9	63
			21	14.9	31.2		4.9	62
			24	14.9	31.3	7.1	5.0	62
Section IV Station 1 (high tide)	44	8	0	16.0	30.7	6.9	5.7	73
			6	15.8	30.8		5.5	69
			12	15.7	30.8		5.1	64
			18	15.1	31.3		5.0	64
			24	15.0	31.2		5.2	66
			30	14.8	31.4		5.3	68
			36	14.6	31.4		5.3	66
			42	14.5	31.5	7.2	5.5	68
Section IV Station 2 (low tide)	44	6	0	15.8	30.9	7.0	4.9	62
			3	16.0	30.9		4.6	59
			6	15.3	31.3		4.9	62
			9	15.1	31.5		5.1	64
			12	15.0	31.6		5.1	64
			15	15.0	31.5		5.1	64
			18	15.0	31.5		5.1	64
			21	15.0	31.5		5.1	64
			24	15.0	31.5	7.0	5.1	64
Section IV Station 2 (high tide)	43	8	0	16.3	30.7	7.0	5.3	69
			6	16.2	30.7		5.3	69
			12	15.9	30.6		5.4	68
			18	15.7	30.8		5.4	68
			24	15.2	31.3		4.6	59
			30	14.6	31.2		4.3	55
			36	14.5	31.4		4.6	58
			42	-	-	7.1	4.0	-

Table B-1 (Cont'd)

	Water Depth, Feet	Secchi Disc, Feet	Depth, Feet	Temp., C	Salinity (0/00)	pH	O, ppm	O Sat., %
Section V Station 1 (low tide)	42	8	0	15.8	30.6	7.0	5.3	68
			3	15.8	30.7		4.8	61
			6	15.6	30.8		4.7	61
			9	15.6	30.9		4.7	61
			12	15.5	30.9		4.6	59
			15	15.3	31.0		4.5	57
			18	15.1	31.0		4.3	54
			21	15.1	31.0	7.0	4.7	59
Section V Station 1 (high tide)	44	8	0	15.7	30.7	7.0	5.6	71
			6	15.8	30.7		5.7	73
			12	15.6	30.9		5.2	66
			18	15.3	31.0		4.9	63
			24	15.1	31.0		5.2	66
			30	14.8	31.2		5.3	68
			36	14.7	31.2		5.2	68
			42	-	31.2	7.4	5.3	-
Section V Station 2 (low tide)	42	8	0	15.6	30.7	7.0	5.0	64
			3	15.7	30.8		4.6	59
			6	15.6	30.8		5.0	64
			9	15.4	30.9		5.1	64
			12	15.2	31.0		5.3	68
			15	15.1	31.1		5.4	69
			18	15.0	31.1		5.4	71
			21	14.9	31.2	7.1	5.3	69
Section V Station 2 (high tide)	42	8	0	15.8	30.7	7.2	5.9	75
			6	15.7	30.7		5.0	64
			12	15.6	30.9		4.5	57
			18	15.4	30.9		4.4	55
			24	15.1	31.0		4.3	55
			30	14.9	31.1		4.3	55
			36	14.6	31.3		4.4	56
			42	-	-	7.0	4.6	-

Table B-2

Environmental Water Quality Data - Part 2

	NH_3^+	$NO_2^- + NO_3^-$	PO_4^-	ΣDiss. P.	Part. P.	ΣP.	Total Coliform Bacteria Cells/100 Ml
	moles/liter						
Section I Station 1 (low tide)	76.0	4.3	0.6	4.0	2.6	6.6	10,000
	29.7	3.4	1.8	4.6	2.6	7.2	1,000
Section I Station 1 (high tide)	86.5	4.6	31.0	33.8	3.8	37.6	500
	35.6	3.7	2.4	13.3	2.8	16.1	3,000
Section I Station 2 (low tide)	23.5	4.4	3.0	4.7	1.1	5.8	7,000
	24.4	5.2	2.6	4.9	1.1	6.0	7,000
Section I Station 2 (high tide)	38.1	4.5	1.6	7.6	3.3	10.9	6,000
	28.6	4.1	2.7	6.7	2.4	9.1	15,000
Section II Station 1 (low tide)	21.9	3.5	2.7	4.1	3.0	7.1	6,000
	14.8	3.4	2.7	3.8	-	-	1,000
Section II Station 1 (high tide)	20.3	4.0	2.1	4.3	3.1	7.4	60,000
	22.1	3.4	3.0	4.2	1.8	6.0	3,000
Section II Station 2 (low tide)	24.8	3.9	2.1	4.5	3.3	7.8	10,000
	20.4	3.9	2.6	4.2	3.3	7.5	600
Section II Station 3 (low tide)	29.1	4.2	2.9	8.3	-	-	4,000
	25.9	4.3	2.3	4.9	1.6	6.5	100
Section II Station 3 (high tide)	18.3	3.4	2.2	3.8	2.2	6.0	6,000
	22.3	3.4	3.4	4.0	1.9	5.9	400

Table B-2 (Cont'd)

	NH_3^+	NO_2^-	NO_3^-	PO_4^-	ΣDiss. P.	Part P.	ΣP.	Total Coliform Bacteria Cells/100 Ml
	moles/liter							
Section III Station 1 (low tide)	23.9	3.7	1.3	4.2	2.2	6.4	30,000	
	20.4	4.0	2.7	3.9	0.6	4.5	4,000	
Section III Station 1 (high tide)	21.1	3.2	2.5	4.3	1.9	6.2	20,000	
	21.2	3.1	3.1	3.9	1.7	5.6	2,000	
Section III Station 2 (low tide)	23.2	3.2	2.2	4.2	2.3	6.5	20,000	
	17.6	3.6	2.6	3.9	1.2	5.1	3,000	
Section III Station 2 (high tide)	20.0	3.8	2.5	4.0	1.5	5.5	10,000	
	20.4	3.4	2.9	3.8	1.3	5.1	3,000	
Section IV Station 1 (low tide)	20.0	3.4	2.8	3.8	3.3	7.1	9,000	
	19.9	3.5	2.8	3.7	0.8	4.5	8,000	
Section IV Station 1 (high tide)	17.1	3.7	2.5	4.1	1.8	5.9	8,000	
	19.9	3.4	2.7	3.7	1.0	4.7	1,000	
Section IV Station 2 (low tide)	19.2	3.3	2.6	3.9	3.2	7.1	50,000	
	18.6	3.5	2.7	3.9	1.7	5.6	7,000	
Section IV Station 2 (high tide)	19.9	3.9	2.5	4.1	1.8	5.9	50,000	
	19.5	2.7	3.0	3.8	1.5	5.3	7,000	
Section V Station 1 (low tide)	18.6	4.1	2.6	4.1	3.9	8.0	50,000	
	19.3	3.6	2.7	3.7	1.3	5.0	30,000	

Table B-2 (Cont'd)

	NH_3^+	NO_2^-	NO_3^-	PO_4^-	Σ Diss. P.	Part P.	ΣP.	Total Coliform Bacteria Cells/100 Ml
	moles/liter							
Section V Station 1 (high tide)	14.4	4.0	2.7	3.5	1.3	4.8		20,000
	17.6	3.2	2.6	3.5	-	-		7,000
Section V Station 2 (low tide)	16.5	3.7	2.5	4.1	0.9	5.0		20,000
	15.3	3.4	2.6	3.6	1.2	4.8		12,000
Section V Station 2 (high tide)	16.2	3.9	2.8	4.0	-	6.8		400
	15.9	3.3	2.7	3.6	-	-		4,000

Table B-3

Benthic Invertebrate and Sediment Data

	No. of Organisms, No/m²	Wet Wt. Organisms, gr/m²	Dominant Organisms(s)	Sediment
Section I				
Station 1				
Grab A	0	0	-	Black silt, H2S
Grab B	0	0	-	Black silt, H2S
Station 2				
Grab A	0	0	-	Black silt, H2S
Grab B	0	0	-	Black silt, H2S
Station 3				
Grab A	650	6.25	Nephytys incisa Polydora ciliata	Clay
Grab B	0	0	-	Black silt, H2S
Station 4				
Grab A	175	3.50	Capitella gracilis	Clay
Grab B	0	0	-	Pebbles, gravel, shell, H2S
Station 5				
Grab A	0	0	-	Sandy silt, H2S
Grab B	0	0	-	Sandy silt, H2S
Section II				
Station 6				
Grab A	28,325	3,480.75	Mytilus edulis	Shells, cobbles
Grab B	85,850	4,679.59	Mytilus edulis	Shells, cobbles
Station 7				
Grab A	0	0	-	Black silt, H2S
Grab B	0	0	-	Black silt, H2S
Station 8				
Grab A	4,525	23.75	Capitella gracilis	Black silt
Grab B	2,025	15.25	Capitella gracilis Polydora ciliata	Black silt
Station 9				
Grab A	850	9.75	Capitella gracilis	Black silt
Grab B	0	0	-	Black silt, H2S
Station 10				
Grab A	0	0	-	Black silt, H2S, oil
Grab B	0	0	-	Black silt, H2S, oil
Section III				
Station 11				
Grab A	0	0	-	Black silt, H2S, oil
Grab B	10,025	153.25	Capitella gracilis	Black silt, H2S, oil
Station 12				
Grab A	100	1.50	Capitella gracilis	Black silt, H2S, oil
Grab B	1,050	27.75		Black silt, H2S, oil
Station 13				
Grab A	2,350	51.00	Capitella gracilis	Black silt, H2S, oil
Grab B	1,100	22.25	Capitella gracilis	Black silt, H2S, oil
Station 14				
Grab A	2,475	36.75	Capitella gracilis	Black silt, H2S oil
Grab B	1,750	26.25	Capitella gracilis	Black silt, H2S oil
Station 15				
Grab A	775	8.75	Capitella gracilis	Brown-black silt, oil
Grab B	1,050	26.25	Capitella gracilis	Brown-black silt, oil

Table B-3 (Cont'd)

	No. of Organisms, No/m²	Wet Wt. Organisms, gr/m²	Dominant Organisms(s)	Sediment
Section IV				
Station 16				
Grab A	8,775	110.25	Capitella gracilis	Brown-black silt, oil
Grab B	7,200	86.25	Capitella gracilis	Brown-black silt, oil
Station 17				
Grab A	1,825	17.50	Capitella gracilis	Brown-black silt, oil
			Polydora ciliata	Brown-black silt, oil
Grab B	3,925	26.25	Capitella gracilis	Brown-black silt, oil
			Polydora ciliata	
Station 18				
Grab A	300	1.50	Capitella gracilis	Brown-black silt, oil
Grab B	975	2.25	Capitella gracilis	Brown-black silt, oil
			Polydora ciliata	
Station 19				
Grab A	6,200	89.75	Capitella gracilis	Brn-blk silt,gravel,oil
Grab B	6,625	103.75	Capitella gracilis	Brn-blk silt,gravel,oil
Station 20				
Grab A	4,125	6.75	Capitella gracilis	Brn-blk silt,gravel,oil
			Polydora ciliata	
			Phyllodoce mucosa	
Grab B	2,375	39.00	Capitella gracilis	Brn-blk silt,gravel,oil
Section V				
Station 21				
Grab A	1,000	5.50	Polydora ciliata	Sand,brn-blk silt,
			Nephtys incisa	grease,oil
Grab B	1,050	3.75	Polydora ciliata	Sand,brn-blk silt
Station 22				
Grab A	2,900	11.50	Polydora ciliata	Sand,blk silt, green clay, oil
Grab B	1,825	4.75	Polydora ciliata	Sand,blk silt, green
Station 23				
Grab A	4,350	6.75	Polydora ciliata	Sand,blk silt, green
			Ophelia sp.	clay, few pebbles
Grab B	1,525	3.00	Polydora ciliata	Sand,blk silt, green
			Nereis sp.	
			Ophelia sp.	
			Phyllodoce greenlandica	
Station 24				
Grab A	650	3.75	Nereis sp.	Sand,gravel,cobbles,H2
			Phyllodoce muscosa	
			Phyllodoce greenlandica	
Grab B	1,625	6.50	Polydora ciliata	Sand,gravel,cobbles,H2
			Capitella gracilis	
			Nereis sp.	
Station 25				
Grab A	550	4.00	Capitella gracilis	Brown layer over black
			Polydora ciliata	silt, oil
			Phyllodoce musocosa	
Grab B	400	28.00	Nereis sp.	Brown layer over black
			Polydora ciliata	silt, oil

Table B-4

Fish Biology Data

Section III

Winter flounder, Pseudopleuronectes americanus

Size, mm	Weight, gm	Age	Sex and Maturity	Stomach Contents
112	32	1+	Imm.	Worms, soot? well-digested
132	47	1+	Imm.	Worms, soot? well-digested
160	167	2+	Ripening female	Algae, 2 shrimps, hydroids, soot, few worms
193	153	2+	Ripening female	Empty

Section IV

Winter flounder, Pseudopleuronectes americanus

Size, mm	Weight, gm	Age	Sex and Maturity	Stomach Contents
59	5	0+	Imm.	Mud, soot, worms
73	9	0+	Imm.	Mud
85	12	0+	Imm.	Worms, soot
104	23	0+	Imm.	Worms, mud
104	25	0+?	Imm.	Empty, little soot
128	47	1+	Imm. female	Worms, soot, mussel
157	92	2+	Ripening female	Worms, mud, detritus, soot
173	115	2+	Male	Many red worms, soot, mud
	fins of this fish heavily parasitized			
176	131	2+	Ripening female	Soot, algae, worms, mud well-digested
	fins lightly parasitized			
195	171	2+	Male	Soot, algae, worms, mud well-digested
	fins lightly parasitized			

Section V

Winter flounder, Pseudopleuronectes americanus

Size, mm	Weight, gm	Age	Sex and Maturity	Stomach Contents
117	39	1+	Imm.	Empty
170	97	2+	Male	Algae, mud, worms, mussel
209	215	3+	Ripening female	Little algae, sea squirts
280	436	4+	Ripening female	Algae, sea squirt
	many parasites on gut			

Ocean pout, Macrozoarces americanus

Size, mm	Weight, gm	Age	Sex and Maturity	Stomach Contents
235	73	3+	Ripe female, few eggs	Empty
275	113	3+	Ripe female, many eggs	Empty

NOTE: All lengths are "standard length" = tip of snout to end of hypural plate. Ages of flounders determined by reading scales, ages of ocean pouts from otoliths. All fishes appeared to be in good condition.

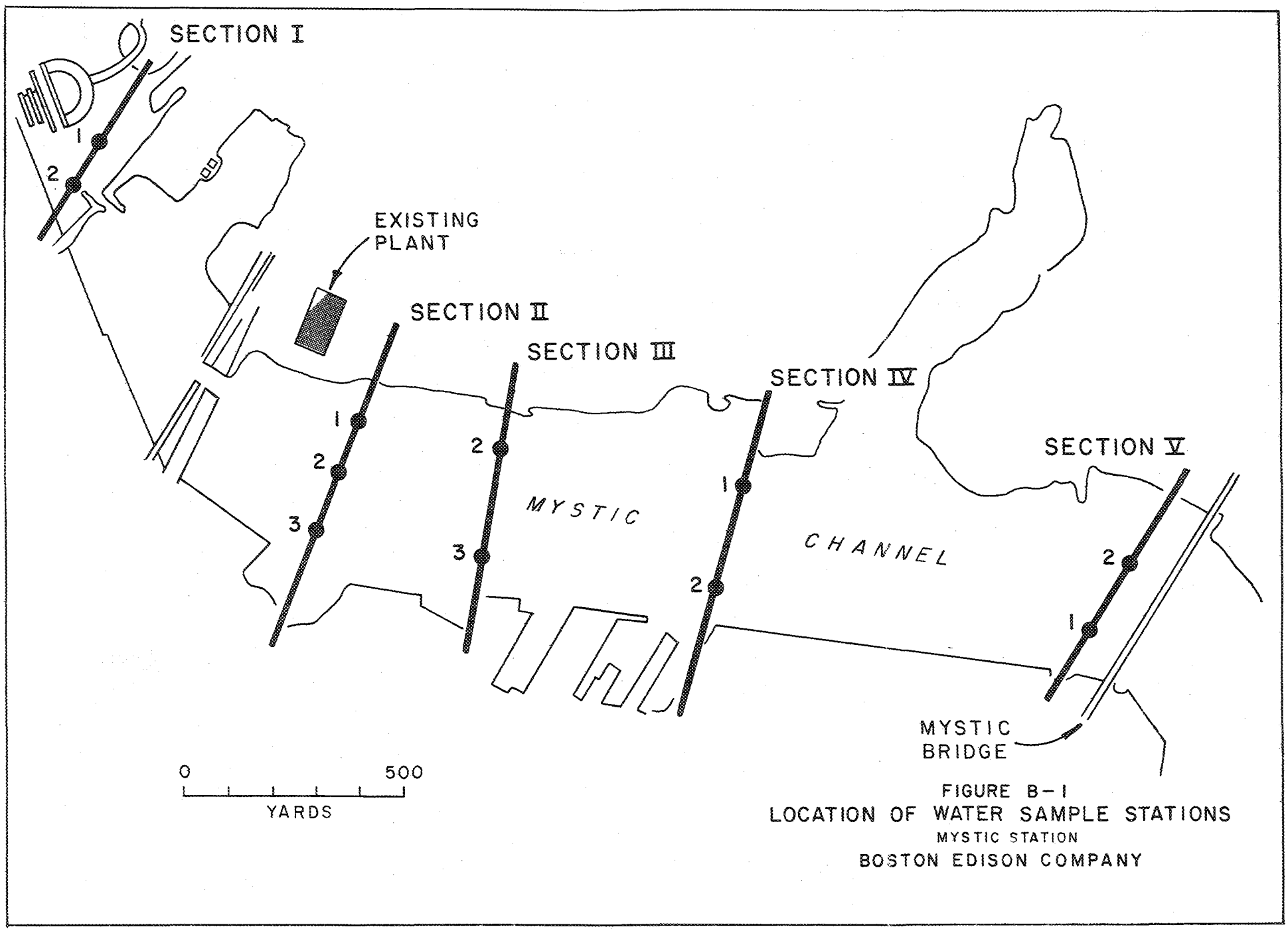

FIGURE B-1
LOCATION OF WATER SAMPLE STATIONS
MYSTIC STATION
BOSTON EDISON COMPANY

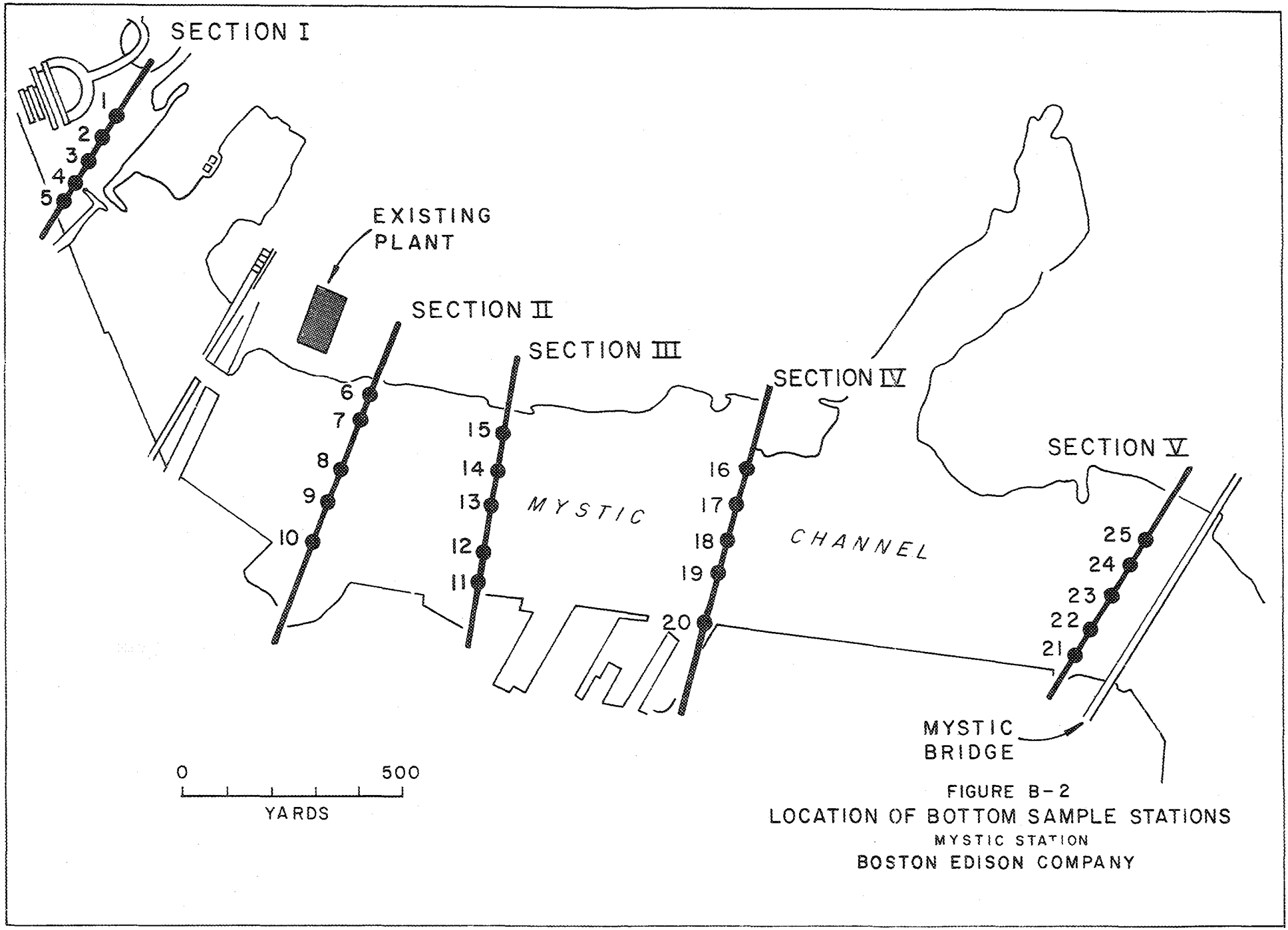

FIGURE B-2
LOCATION OF BOTTOM SAMPLE STATIONS
MYSTIC STATION
BOSTON EDISON COMPANY

APPENDIX C

HYDROTHERMAL FIELD SURVEY

MYSTIC STATION

BOSTON EDISON COMPANY

STONE & WEBSTER ENGINEERING CORPORATION

NOVEMBER 1970

TABLE OF CONTENTS

I. INTRODUCTION AND OBJECTIVES

In connection with the proposed new unit at Mystic Station, a comprehensive field survey was conducted in the Mystic channel in the plant vicinity.

The objective of this survey is to provide data which, together with information from a separate ecological study, will form the basis for selecting a design concept of the new circulating water intake and discharge structures. Predictions regarding hydrothermal conditions generated by the expanded plant with the design concept will be made using this field data.

To obtain the data required for a complete understanding of present hydrothermal conditions, the following types of measurements were made:

1. Bottom topography

2. Current patterns

3. Temperature profiles

4. Dye recirculation study

In addition, plant operating data and meteorological information were obtained during the field survey.

This report describes the scope and techniques of the comprehensive field survey and summarizes the data in graph form. An evaluation of the data and a description of the mechanism by which water flows into and out of the site area are given. A future report will present the concept of the circulating water intake and discharge structures for the new unit, and present the corresponding predicted hydrothermal patterns.

II. SITE AND PLANT DESCRIPTION

Boston Edison's Mystic Station is located on the north bank of the Mystic River channel, Everett, Massachusetts, approximately 1.1 miles upstream from the Tobin Bridge and approximately 5 miles upstream from the inner harbor entrance at Castle and Governor's Islands. Figure C-1 shows the plant location, just downstream from the Alford Street Bridge. The Amelia Earhart Lock and Dam is approximately 0.5 miles upstream from the plant. There is negligible fresh water flow through the dam. Thus, the Mystic channel downstream from the dam has effectively a dead end, and the only natural flow at the plant site is due to tides.

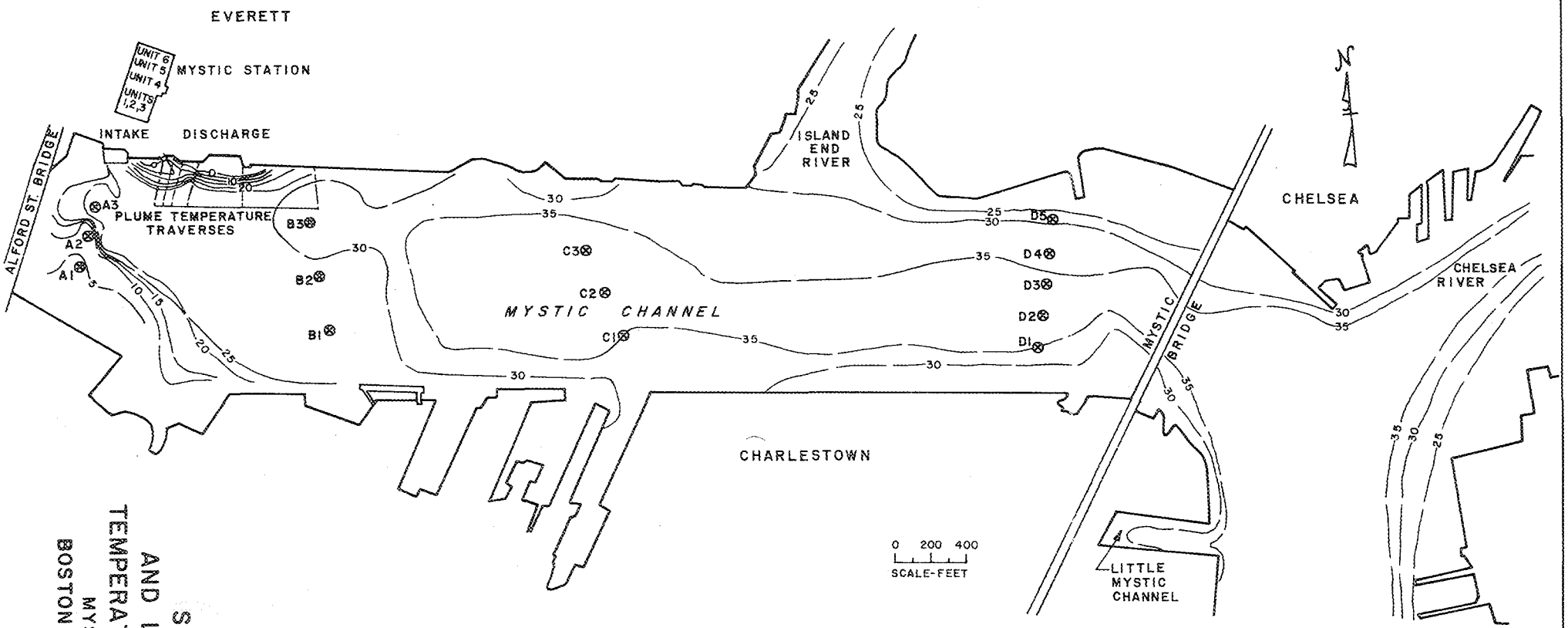

NOTE:

1. DEPTH CONTOURS ARE FEET BELOW LOW WATER DATUM.
   SUBTRACT 0.78 FEET TO CONVERT TO BOSTON CITY BASE.
2. ⊗ TEMPERATURE PROFILE STATIONS

FIG. C-1

SITE PLAN
AND LOCATION OF
TEMPERATURE TRAVERSES
MYSTIC STATION
BOSTON EDISON COMPANY

The range of tide at the plant varies between 6.0 and 13.5 feet with a mean 9.4 feet. With this mean tide range, the average flood or ebb flow at the plant site is approximately 1,000 cfs. At the plant, the Mystic channel is approximately 1,100 feet wide, and the depth varies from 0 to approximately 30 feet.

The present Mystic Station consists of six oil-fired units with a total installed capacity of 618 MW. Units 1, 2, and 3 are each rated at approximately 50 MW and Units 4, 5, and 6 are each rated at approximately 159 MW.

The general plant layout and details of the circulating water system are shown in Figure C-2. Condenser cooling water is taken from the Mystic channel by the intake structure and circulating water pumps, passed through the condensers where it picks up rejected plant heat, and returned to the channel by a common discharge canal. Each condenser is divided into two separate sections, with temperature sensors on the downstream side of all sections. The average temperature rise through the plant is 18 F at rated load.

The intake structure for each unit consists sequentially of a trash rack, curtain wall, traveling screen, and circulating water pump. All units have one pump, with the discharge lines of Units 1-3 manifolded and those of Units 4-6 manifolded. In

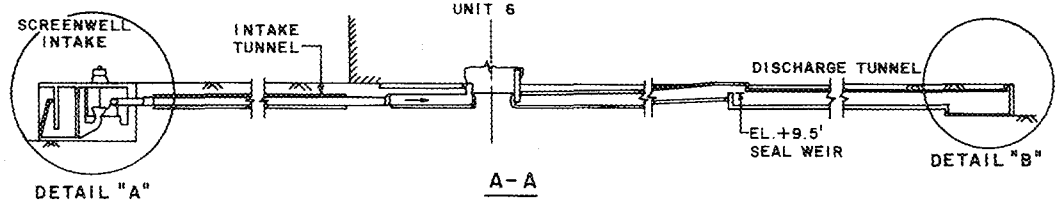

A-A

0 25 50
SCALE-FEET

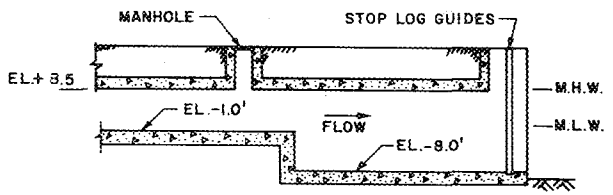

DETAIL "B" DISCHARGE STRUCTURE

0 10 20
SCALE-FEET

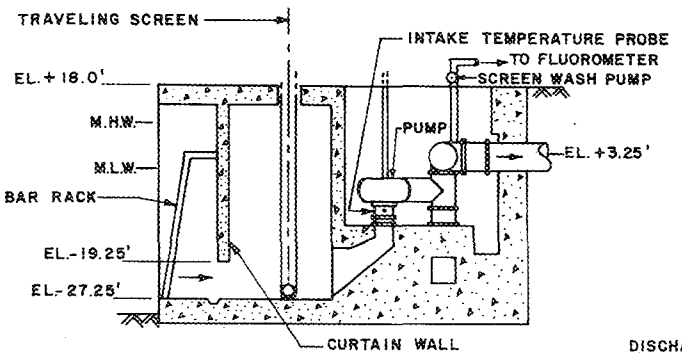

DETAIL "A" INTAKE STRUCTURE

0 10 20
SCALE-FEET

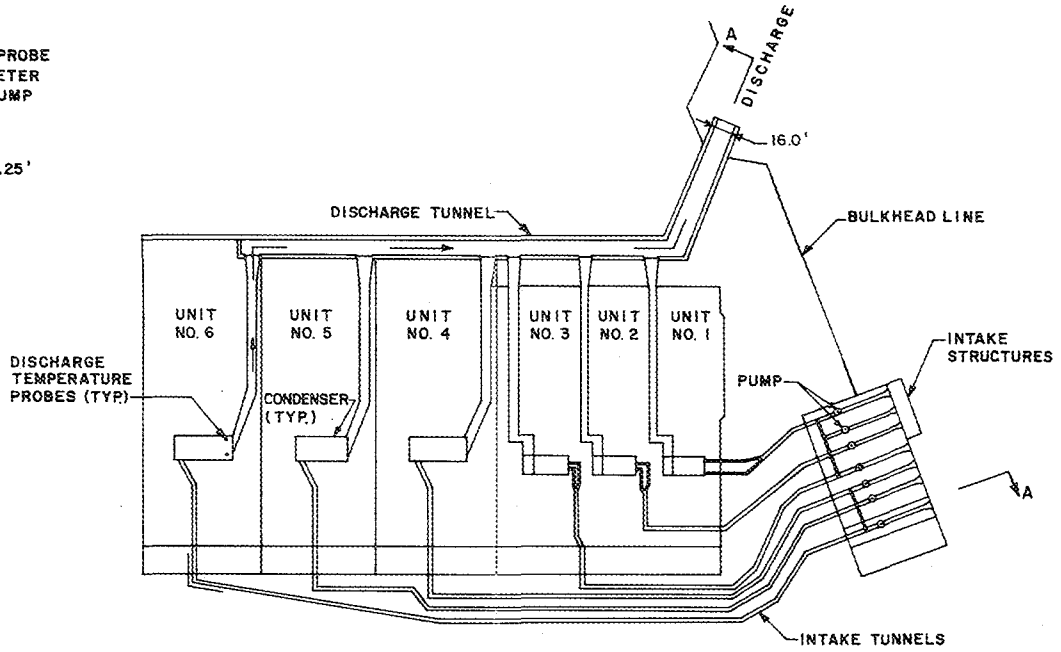

PLAN

0 25 50
SCALE-FEET

NOTE:
1. ELEVATIONS REFERENCED TO BOSTON CITY BASE.

FIG. C-2

CIRCULATING WATER SYSTEM
INTAKE & DISCHARGE STRUCTURES
MYSTIC STATION
BOSTON EDISON COMPANY

addition, there is one spare pump for Units 1-3. The total design flow from the six main pumps is 780 cfs.

The discharge structure shown in Figure C-2 is basically a free surface tunnel ending in a single opening, located approximately 300 feet downstream from the intakes. The tunnel is 16 feet wide, the invert of the opening is at El. -8.0, and the free surface flow is discharged downstream at a 45 degree angle with the bulkhead line. Water levels in the tunnel depend on the tide. However, each unit has a seal weir at the junction of the individual unit discharge canal and the common discharge tunnel. Since the crest of each seal weir is at El. +9.5, the pressure heads at the individual unit discharge weirs are not affected, except at high tide stages. Flow through the circulating water pumps, therefore, varies primarily as a function of tide induced head changes at the intake. At high tide, the static head is less than at low tide, and the flow at high tide is, therefore, somewhat greater.

III. FIELD SURVEY PROGRAM

This section presents in more detail the scope and techniques used to measure the following site and plant characteristics:

a. Plant operating data

b. Meteorology

c. Bottom topography

d. Tide water levels

e. Temperature profiles

f. Current patterns

g. Dye recirculation from plant discharge

a. Plant Operating Data

To determine the effect of plant operation during the survey on the hydrothermal field conditions, measurements were made of gross plant output, circulating water intake temperature, and the

corresponding discharge temperature. In addition, the number of operating circulating water pumps was noted.

Gross plant output or load is an average value of power generated by all plant units during a given hour of operation. This is recorded routinely by the plant recorder.

Intake temperatures were continuously measured by a standard plant thermistor immersed in a tank, especially set up for the survey, which continuously received water from the suction lines of Units 4 and 5 circulating water pumps. Figure C-2 shows the location of the sampling points on the pumps.

Discharge temperatures were continuously measured by standard plant thermistors on the downstream side of each split condenser. Therefore, there are a total of 12 thermistors measuring discharge temperatures. The plant discharge temperature was determined by averaging the temperatures recorded for the operating units, weighted according to the flow rates for each unit. Figure C-2 shows the location of the discharge temperature sensors.

Both the intake and discharge temperatures were recorded every four minutes by the plant recorder, which truncates the decimal fraction of a degree. All sensors were calibrated against mercury thermometers, and data reported are the corrected values.

b. Meteorology

This data was collected to evaluate effects of wind on drogue floats used for the current survey and to compute the heat transfer from the water surface to the atmosphere. The meteorological data consisted of wind velocity, air temperature, relative humidity and cloud cover collected from Logan Airport.

c. Bottom Topography

Knowledge of water depths was required to evaluate flow patterns and the variation of temperatures with tide. Water depths were measured in the Mystic channel along a number of traverses from a boat equipped with a commercial side-scan sonar system. This system consisted of a tow "fish," acoustic energy source and graphic strip chart recorder. Depths in the discharge plume were determined from soundings during the plume

temperature survey. All water depth measurements were corrected for tidal stage and are reported as depths below low water datum.

d. Tide Water Levels

Tide stage was measured at the Mystic Station by periodic readings of the plant tide staff gage and by continuous recording using a commercial water level recorder. The continuous recorder and staff gage were referenced to Boston City Base. During the week of the dye recirculation study, the continuous recorder was not used.

e. Temperature Profiles

Vertical temperature profiles were measured at numerous positions, both in the plant discharge plume and in the Mystic channel. Some additional profiles were also measured in Boston Harbor. In general, measurements were made at depths of 1, 5, 10, 15, etc., to the bottom. All data was recorded using weighted thermistor probes lowered from boats, and positioned at the given depths for sufficient time such that data recorded on strip charts had reached steady-state. The thermistors

were calibrated before and after the survey and were compared to the plant intake temperature probe by making simultaneous measurements of intake water from the pump suction lines. All temperature measurements were made over a complete tidal cycle on September 18.

The location of the temperature measurements is shown in Figure C-1. For measurements in the discharge plume, a number of traverses were established, along which vertical profiles were taken at sufficient stations to define the plume temperatures. Temperature profiles in the Mystic channel were taken at the designated stations along traverses A through D. At each of these traverses, the extreme positions such as B1 and B3, were marked with buoys. Position of the buoys was determined by triangulation from the shore, whereas position between the buoys was estimated by personnel in the boats.

f. Current Patterns

Current patterns were observed to determine the origin of the colder ambient water required for the plant intake and for the discharge plume dilution mechanism, and to determine the destination of the warmer plant discharge.

Current patterns were measured by releasing 10 drogues in the water and following their movement by triangulation from two points on the shore. The drogues consisted of small parachutes suspended either 5 feet or 20 feet below small surface floats. Since the drag of the surface marker floats was relatively negligible, the drogues moved with the current at the depth of the parachutes. All current measurements were made during a complete tidal cycle on September 17.

g. Dye Recirculation

The dye tracer study was conducted to determine the amount of condenser water recirculation from the plant discharge to the intake, since recirculation can affect the temperatures of the discharge plume.

To test for recirculation, rhodamine WT dye was injected at a predetermined rate into the discharge canal. Dye concentration in the intake was continuously monitored over a five-day period, September 28, to October 2, 1970. The percentage recirculation was determined from the ratio of the intake dye concentration to the discharge dye concentration. The program was scheduled to extend over a sufficient period

so that a steady-state condition could be reached. Thus, the intake dye concentration would eventually repeat in a cyclical manner with the tidal cycle. After steady-state had existed for several days, dye injection was stopped to determine if the Mystic channel water would return to the initial level of background dye concentration. Dye injection was begun at 0915 on September 28, and stopped at 0750 on October 1.

The number of circulating water pumps in operation was monitored so that the dye injection rate could be adjusted to produce a constant dye concentration with time in the discharge canal. However, during the entire survey, all six of the main circulating water pumps and the spare pump were operating. The total flow through the plant was computed from pump curves to be 875 cfs, except for tidal induced variations.

Dye was injected into the discharge canal using a chemical proportioning pump with an adjustable injection rate. The pump was calibrated at the site and was accurate to 0.01 liter per hour. Methanol was added to a 20 percent rhodamine WT dye solution to bring the solution to the specific gravity of sea water. The addition of methanol provided a dye-alcohol solution

containing 0.309 pounds of pure dye per liter. Dye was injected at 5.89 liter per hour, which together with the above plant flow yielded a discharge concentration of nine parts per billion (ppb).

The dye concentration at the intake structure was monitored with a commercial continuous recording fluorometer. A screen backwash pump was used to pump intake water from the manifold downstream of pumps for Units 4-6 to a tank on the upper deck of the screenhouse. Sufficient water was pumped so that the retention time for water in the tank was approximately 15 minutes. Before flowing through the fluorometer from the tank, the water temperature was measured with a mercury thermometer to allow temperature corrections of the fluorometer readings.

Since all water has some natural background fluorescence, the fluorometer was calibrated over a two-day period before the start of dye injection. This determined the proper filters to use so as to account for the natural fluorescence of Mystic River water.

During the dye recirculation study, hourly tidal readings were made from a staff gage which had been calibrated

during the temperature and current survey. Hourly temperature profiles were also taken in front of the intake structure with a commercial thermocouple.

Grab samples were taken from the discharge canal downstream of the dye injection point in order to check the discharge dye concentrations.

IV. PLANT OPERATING DATA

Illustration of plant operating data is separated into two categories:

a. During the two days of the current and temperature pattern survey

b. During the week of the dye recirculation study

Figure C-3 shows the gross plant load, hourly average discharge temperature, and plant intake temperature during the current and temperature survey, September 17 and 18. After 10:A.M. on September 17, the plant load remained approximately at 520 MW, except for some load decrease around midnight. Currents and temperatures, measured during the daylight hours were, therefore, surveyed with the plant at 520 MW.

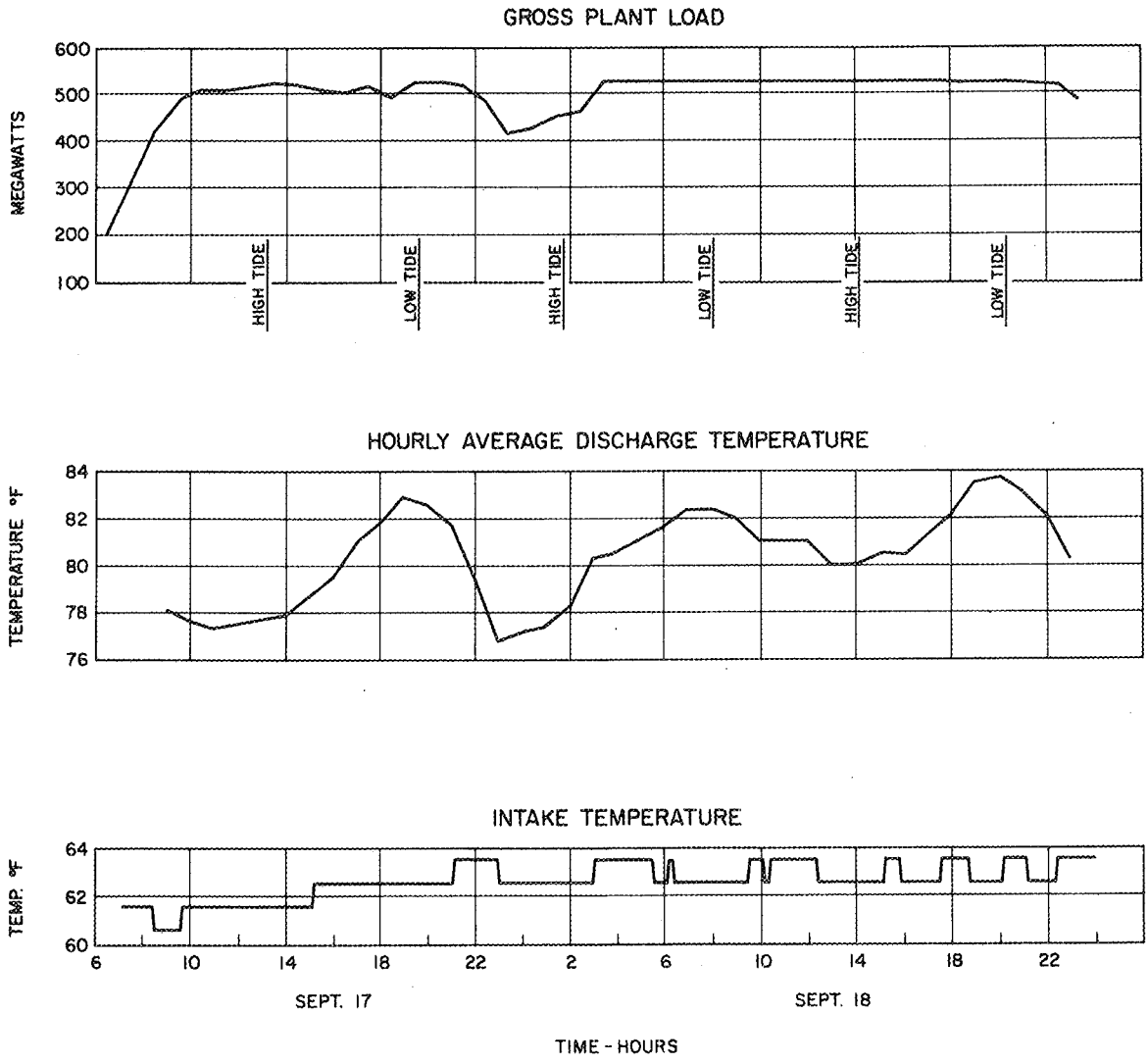

NOTES:

1. DISCHARGE TEMPERATURES DETERMINED FROM CONDENSER OUTLET SENSORS ON ALL UNITS.
2. INTAKE TEMPERATURE DETERMINED FROM ONE SENSOR SAMPLING TWO PUMP SUCTION LINES.

FIG. C-3

PLANT LOAD AND CIRCULATING WATER TEMPERATURES
SEPT. 17 & 18, 1970

MYSTIC STATION
BOSTON EDISON COMPANY

MSO-RH

The temperature of the plant discharge water is shown to vary both with plant load and with the tide. At high tide, the discharge temperature is lower than the temperature at low tide, although the plant load is essentially constant. This temperature variation is due to the head change on the pumps and the corresponding change in flow rate. The free water surface elevation downstream from the pumps is controlled by seal pits with weir crests at El. +9.5. Thus, a higher water surface at the intake reduces the head on the pumps, resulting in a higher flow rate and a lower temperature rise through the condensers. During the temperature survey, the plant dishcarge temperature varied from approximately 80 to 82 F.

Plant intake temperatures showed a slight upward trend during September 17. During September 18, the intake temperatures were essentially constant. The "step like" variation of the intake temperature record is due to the plant recording system which truncates fractions of a degree. A temperature change as small as 0.1 F can produce a recorded 1.0 F temperature change. The average intake temperature during the September 18 temperature survey was approximately 63 F.

Figure C-4 shows the gross plant load and intake temperature during the week of the dye recirculation study, September 28, through October 2. Except for load reductions during the nights,

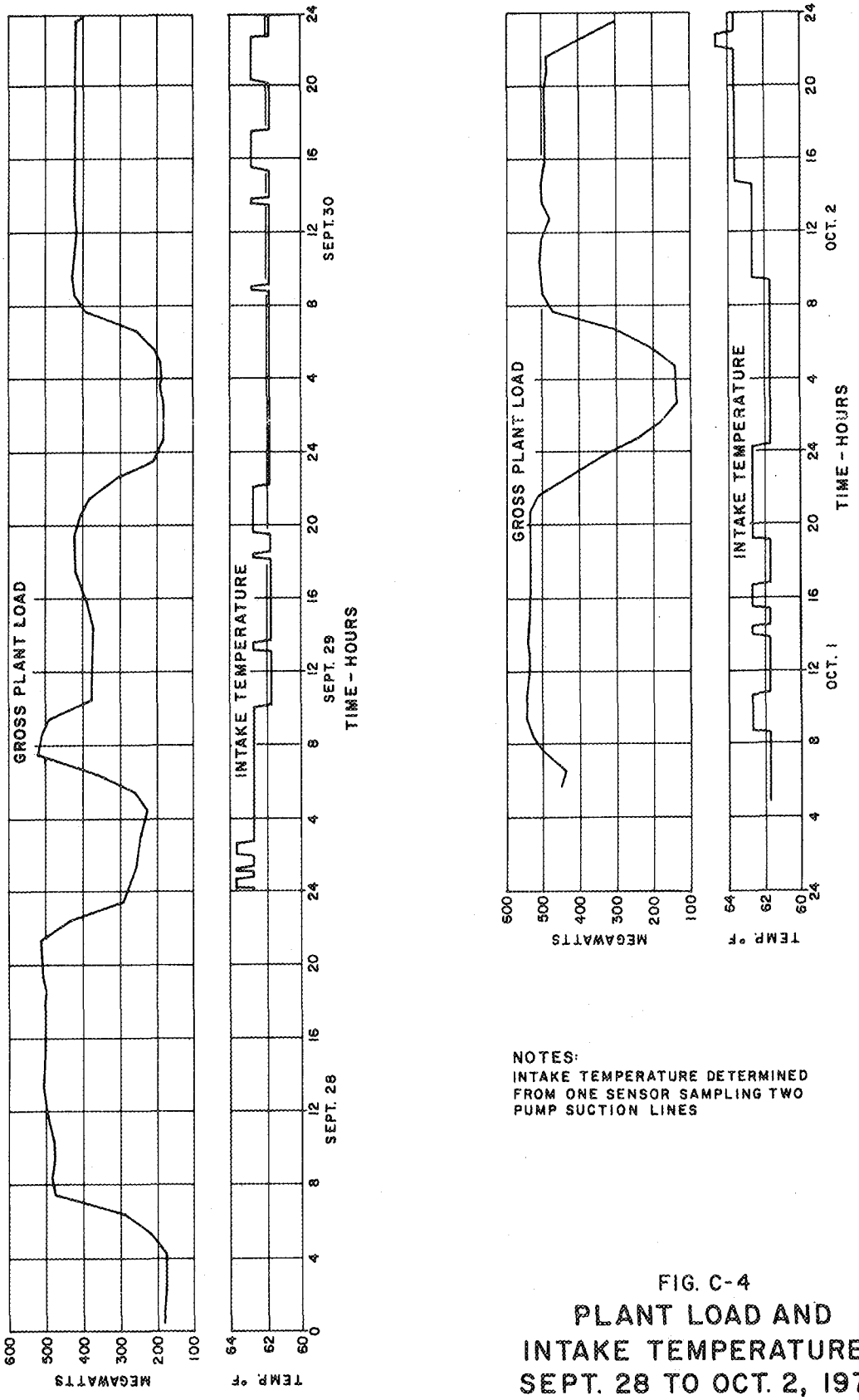

NOTES:
INTAKE TEMPERATURE DETERMINED FROM ONE SENSOR SAMPLING TWO PUMP SUCTION LINES

FIG. C-4

PLANT LOAD AND INTAKE TEMPERATURES SEPT. 28 TO OCT. 2, 1970

MYSTIC STATION
BOSTON EDISON COMPANY

plant load was maintained between approximately 400 and 500 MW throughout the entire dye recirculation study. The intake temperature was essentially constant at approximately 62 F, except for an increase to approximately 63 F during the last day of the recirculation study, October 2.

V. SURVEY DATA AND EVALUATION

This section summarizes the field data in graph form and presents a description of the meteorological conditions during the current and temperature survey. An evaluation of the data is made as it is presented.

A. Meteorology

During the current pattern survey on September 17, the sky was clear. Winds were light, averaging approximately 10 mph, and varying from the north in the morning, through east, to southerly in the evening. The average air temperature was 63 F and the average relative humidity was approximately 60 percent. These conditions were ideal for the current survey since visibility was excellent and the drogues were not affected by the light winds.

During the temperature pattern survey on September 18, the sky was heavily overcast and it occasionally rained. Winds were

light, averaging approximately 10 mph, varying from southerly to southwesterly. The average air temperature was 66 F and the average relative humidity was approximately 95 percent. Due to the low winds and high relative humidity, heat transfer from the water surface was negligible in the Mystic channel.

B. Bottom Topography

Figure C-5 shows depth contours below low water datum in the Mystic channel at the plant site. This information is a combination of data from the fathometer transects in the Mystic channel and from soundings taken near the plant discharge during measurements of plume temperatures. This figure illustrates that the water depths at low water are between 25 and 30 feet in the central portion of the Mystic channel leading to the plant intake. To be noted is the bottom material built up along the bulkhead downstream from the intake. This shelf extends up to the low water datum and is exposed during periods of extreme low tides. Shallow water depths also exist over a large area near the shore opposite the intake.

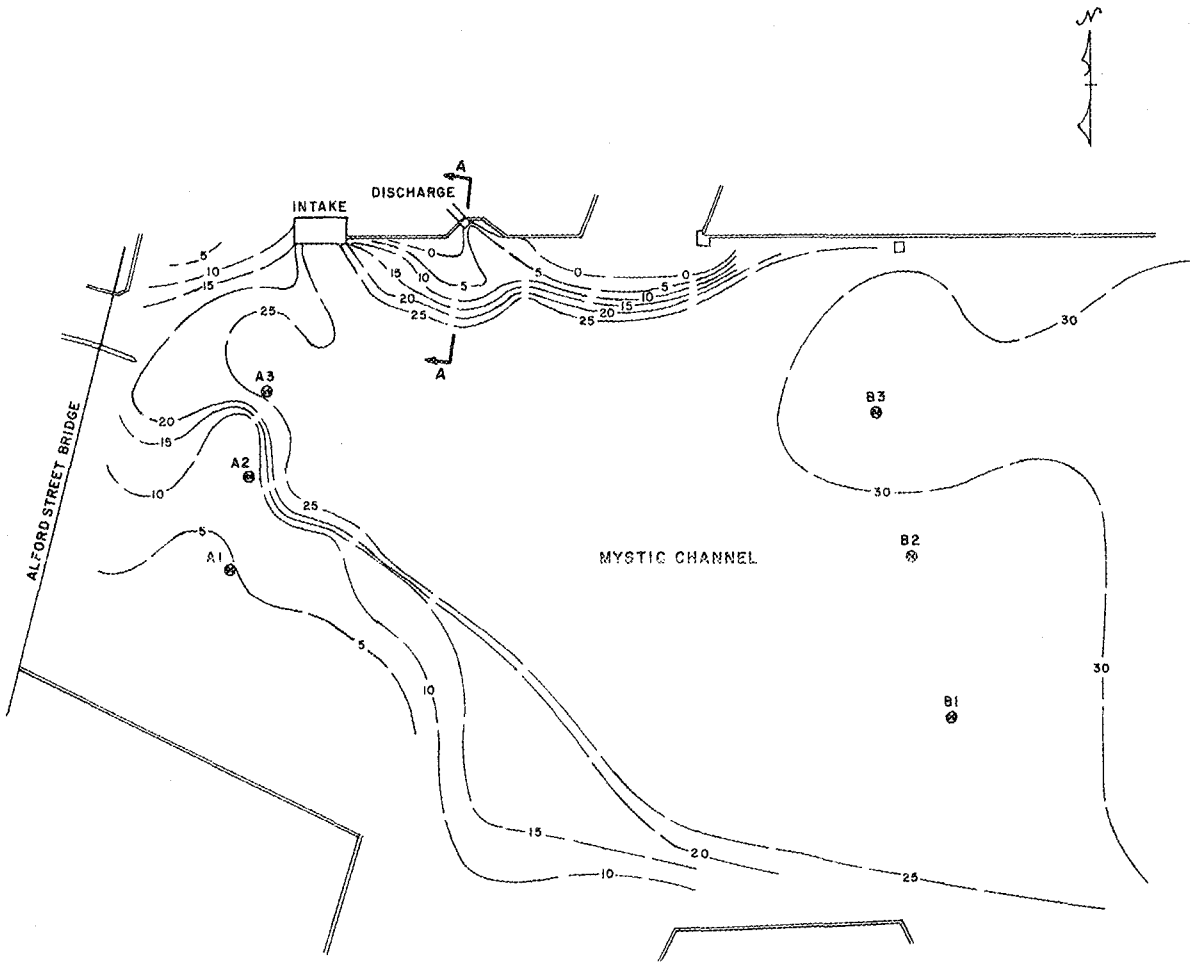

0 100 200 300

SCALE-FEET

NOTES:

1. DEPTH CONTOURS ARE FEET BELOW LOW WATER DATUM. SUBTRACT 0.78 FEET FROM DEPTHS TO CONVERT TO BOSTON CITY BASE.
2. ⊗ TEMPERATURE PROFILE STATIONS

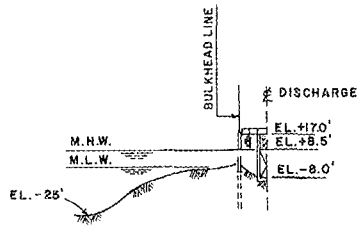

A-A

DISTORTED SCALE
(BOSTON CITY BASE)

FIG. C-5

MYSTIC CHANNEL BOTTOM TOPOGRAPHY AT PLANT SITE

MYSTIC STATION
BOSTON EDISON COMPANY

C. Tide

The water surface variation with time at the plant during the current and temperature survey is shown on Figure C-6. A maximum vertical tidal range of approximately 13 feet occurred during these two days, as compared to the average range of 9.4 feet at the site. It should be pointed out that the survey days were selected to coincide with this high tidal range since it would more clearly demonstrate any effect that the tide has on field conditions. High tide was at 1:15 P.M. during the current survey and at 2:00 P.M. during the temperature survey.

D. Temperatures and Currents

Discharge plume temperature patterns and current patterns in the Mystic channel are illustrated for a period of a few hours near each of three tidal stages:

a. Maximum flood tide

b. High tide

c. Maximum ebb tide

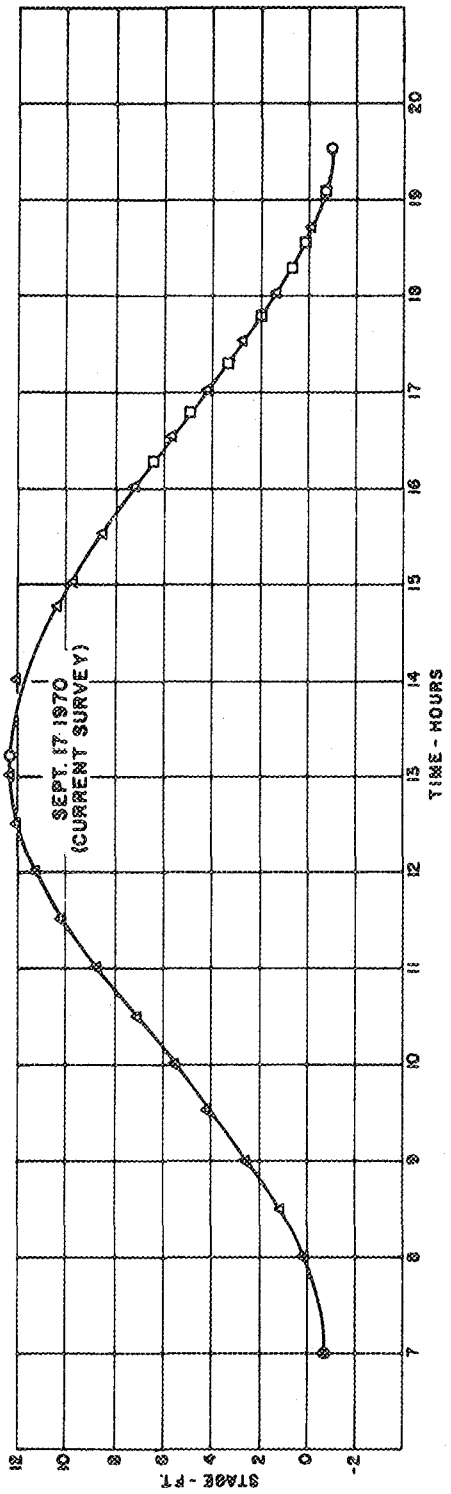

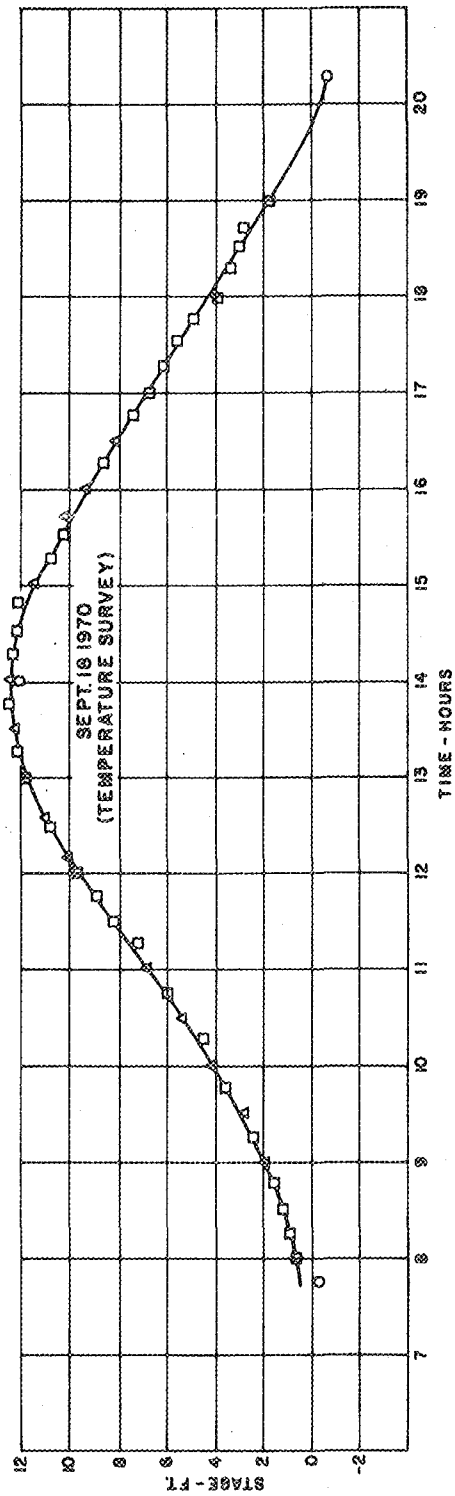

LEGEND:
○ TIDE CHARTS (BOSTON HARBOR)
△ STAFF GAGE AT PLANT
□ RECORDER AT PLANT

NOTES:
1-STAGE REFERENCED TO BOSTON CITY BASE
2-TO CONVERT STAGES TO MEAN LOW WATER DATUM SUBTRACT 0.78 FEET

FIG. C-6
TIDE LEVELS
DURING TEMPERATURE
AND CURRENT SURVEYS
MYSTIC STATION
BOSTON EDISON COMPANY

Data during flood tide represents an average over two to three hours near the maximum strength of flood tide. Similarly, data during high and ebb tides represent averages of a few hours near high tide and near the maximum strength of ebb tide, respectively. The range of tide stage included in each of the three above tidal periods is shown on the respective figures.

a. Flood Tide

Temperatures of the discharge plume as measured 1 foot below the surface during a few hours near maximum flood tide, are shown in Figure C-7. These temperatures are taken to be surface temperatures, and were the maximum recorded in any vertical profile. In addition, vertical temperature traverses are illustrated upstream and downstream from the plume. The temperature pattern indicates a relatively rapid laterial drop in temperature at the river side of the plume boundary as compared to the longitudinal temperature drop along the bulkhead. Although such a relative variation is characteristic of surface jets, this tendency is reinforced by the bottom shelf along the bulkhead shown in Figure C-5. The geometry of the bottom shelf and the temperature contours indicate that most of the entrainment of colder bottom water takes place along the steep slopes of the shelf. The average plant discharge temperature during flood tide was 81.5 F.

NOTES:
1. TEMPERATURES IN °F.
2. TEMPERATURE PROFILES RECORDED WHERE DRAWN.
3. STAGE: +1 TO +7 SEPT. 18, 1970.

FIG. C-7
SURFACE TEMPERATURES IN DISCHARGE PLUME DURING FLOOD TIDE
MYSTIC STATION
BOSTON EDISON COMPANY

MSC-134

The vertical temperature profiles downstream from the plant discharge show that a distinct two-layer flow system was formed with a warmer surface layer flowing over a colder lower layer. Temperature profiles upstream from the discharge show the temperatures to vary more continuously with depth. This, together with the expanding shape of the plume temperature contours, indicates that heat from the plume flowed upstream and mixed with the lower colder water during the flood tide.

Current patterns during the few hours near maximum flood tide are shown in Figure C-8. This figure clearly demonstrates the large eddy which brings some of the discharged water back upstream. Typical eddy velocities in the upper layer for the entire survey varied from 0.2 to 0.4 fps. A combination of the flow rotation and bottom topography probably results in some of the warmer surface water mixing with the colder lower water as it moves upstream. The flow path of the lower layer, shown by the dashed lines in Figure C-8, indicates that the upstream flow of colder water is confined and guided by the channel bottom along the shore opposite the intake and by the shelf along the plant bulkhead. Velocities of the lower layer during the entire survey varied from 0.15 to 0.3 fps.

LEGEND:

- o TRIANGULATED POSITION OF DROGUE
- ----→ L = 20 FEET (LOWER LAYER)
- ——→ L = 5 FEET (UPPER LAYER)

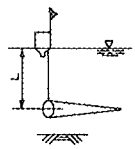

DROGUE DETAIL

NOTES:

1. STAGE: +1' TO +10' SEPTEMBER 17, 1970
2. DEPTH CONTOURS ARE FEET BELOW MEAN LOW WATER DATUM SUBTRACT 0.78 FEET FROM DEPTHS TO CONVERT TO BOSTON CITY BASE.

FIG. C-8

CURRENT PATTERN DURING FLOOD TIDE

MYSTIC STATION

BOSTON EDISON COMPANY

b. High Tide

Plume temperatures measured 1 foot below the surface a few hours during high tide are shown in Figure C-9. A comparison of Figure C-9 with Figure C-7 shows that the plume at high tide is somewhat more confined to the plant side of the Mystic channel and is somewhat lower in temperature than the plume during flood tide. The lower temperatures in the plume are due to two factors. As was mentioned relative to Figure C-3, the plant discharge temperature is lower at high tide due to less head on the circulating water pumps and correspondingly increased circulating water flow. At flood tide, the discharge temperature was an average of 81.5 F while at high tide it was 80.5 F. Secondly, a higher water level reduces the restricting effects of the bottom shelf along the plant bulkhead and therefore allows more lower, colder water to be entrained in the plume.

The temperature profiles in Figure C-9 show that during high tide, the two-layer flow system was maintained upstream as well as downstream from the plant. That is, the warmer water discharged by the plant essentially remained in the surface layer.

Current patterns during the few hours of high tide are shown in Figure C-10. Although the number of drogue positions are fewer

NOTES:

1. TEMPERATURES IN °F.
2. TEMPERATURE PROFILES RECORDED WHERE DRAWN.
3. STAGE: +11 THROUGH HIGH +7.

FIG. C - 9

SURFACE TEMPERATURES IN DISCHARGE PLUME DURING HIGH TIDE

MYSTIC STATION

BOSTON EDISON COMPANY

MSD 14N

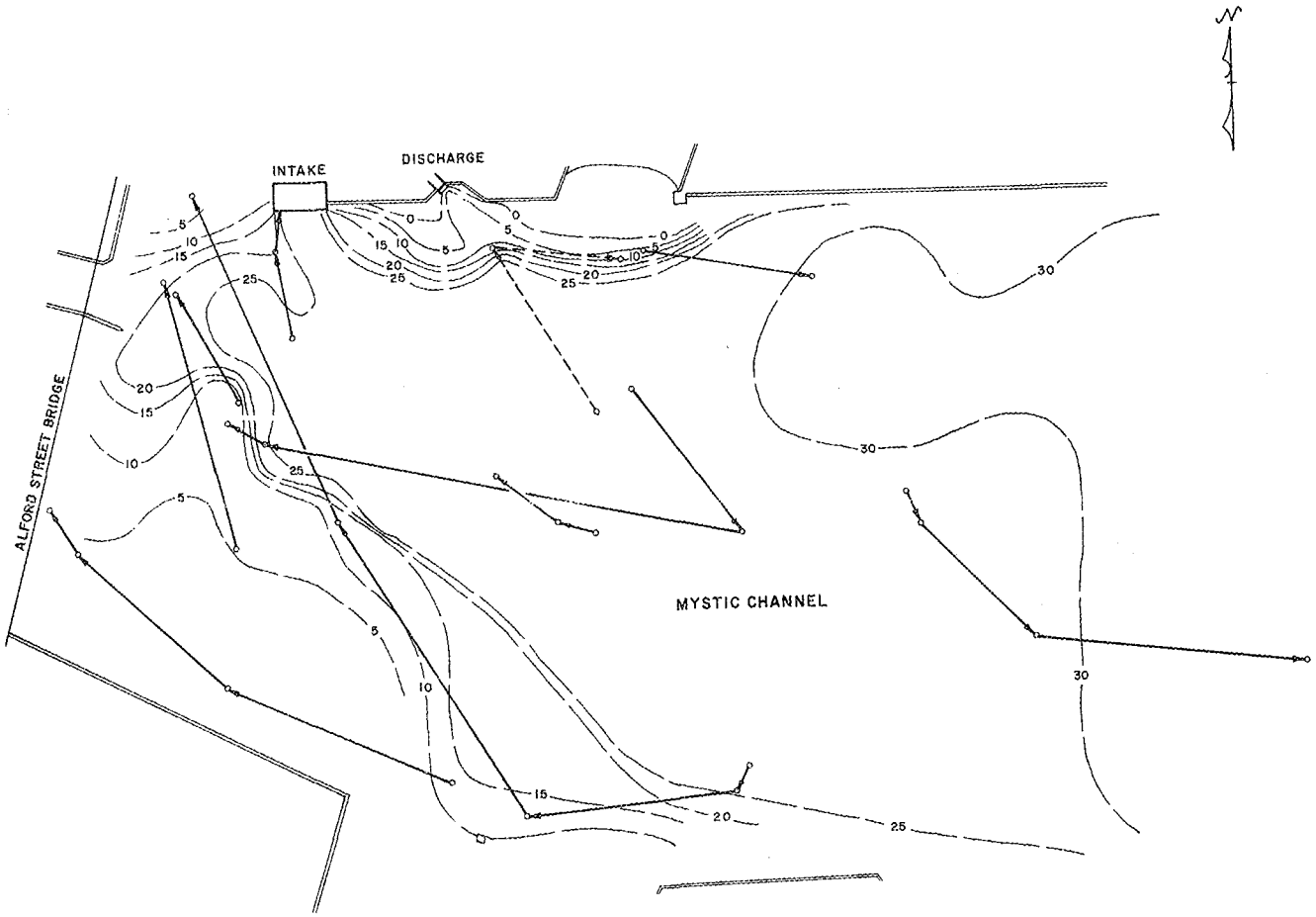

LEGEND:

- o TRIANGULATED POSITION OF DROGUE
- ~~~o L = 20 FEET (LOWER LAYER)
- ——→ L = 5 FEET (UPPER LAYER)

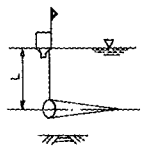

DROGUE DETAIL

NOTES:

1. STAGE: +1' TO + 8' SEPTEMBER 17, 1970
2. DEPTH CONTOURS ARE FEET BELOW MEAN LOW WATER DATUM SUBTRACT 0.78 FEET FROM DEPTHS TO CONVERT TO BOSTON CITY BASE.

FIG. C-10

CURRENT PATTERN DURING HIGH TIDE

MYSTIC STATION

BOSTON EDISON COMPANY

than shown for the flood tide, it seems evident that the large eddy persisted and carried some of the surface flow upstream from the plant intake. Higher water levels, however, prevented mixing of the two flow layers and maintained the warmer surface layer higher above the intake opening than at flood tide. The lower colder layer flow, shown by the dashed path line, was entrained by the plume since the higher water reduced the restricting effect of the bottom shelf near the discharge structure.

c. Ebb Tide

Plume temperatures measured 1 foot below the surface during a few hours near maximum ebb tide are shown in Figure C-11. A comparison of Figure C-11 with Figures C-9 and C-7 shows that although plume temperatures at ebb tide are somewhat warmer than at high tide, the plume at ebb tide is somewhat cooler than during flood tide. The lower water levels of ebb tide in conjunction with the bottom shelf along the plant bulkhead minimize the entrainment of colder bottom water into the jet. Also, the average discharge temperature during ebb tide was 82.5 F, compared to 80.5 F during high and 81.5 F during flood tide. However, plume temperatures during ebb tide are somewhat cooler than during flood tide since more of the heat is carried downstream by the ebb tide current.

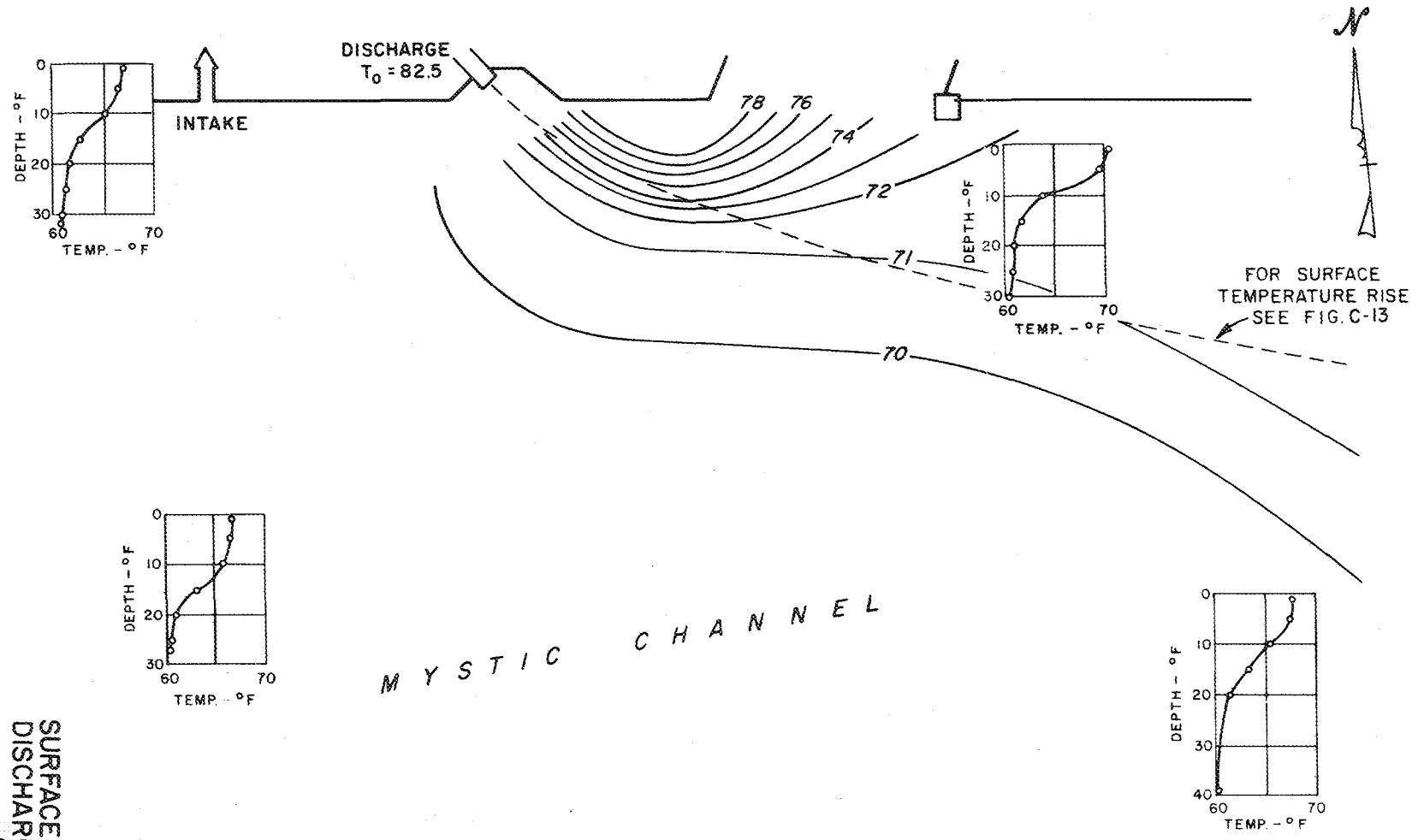

NOTES:

1. TEMPERATURES IN °F
2. TEMPERATURE PROFILES RECORDED WHERE DRAWN.
3. STAGE +5 TO +1 SEPT. 18, 1970.

0 100 200
SCALE - FEET

FIG. C-11

SURFACE TEMPERATURE IN DISCHARGE PLUME DURING EBB TIDE

MYSTIC STATION

BOSTON EDISON COMPANY

Temperature profiles of Figure C-11, during the hours near maximum ebb tide, indicate that the two-layer flow system existed at all points in the Mystic channel. The warm surface layer upstream of the discharge is probably a combination of plant discharge flowing in the weaker eddy during ebb tide, and previously discharged warm water flowing downstream under the Alford Street Bridge.

Current patterns during maximum ebb tide are shown in Figure C-12. As indicated, relatively more of the plant discharge is flowing downstream in the Mystic channel. However, the clockwise eddy also persisted. It should be noted that the colder lower layer, as shown by the dashed flow paths of Figure C-12, flowed upstream even during ebb tide. This upstream flow of colder water is produced by a combination of the plant intake and the entrainment of water into the discharge plume.

d. Surface Temperature Rises

Discharge plume temperatures were summarized in terms of surface temperature rises above ambient by using the plume temperatures along the longitudinal sections shown in Figures C-7, C-9, and C-11, and temperature at Stations C3 and D3.

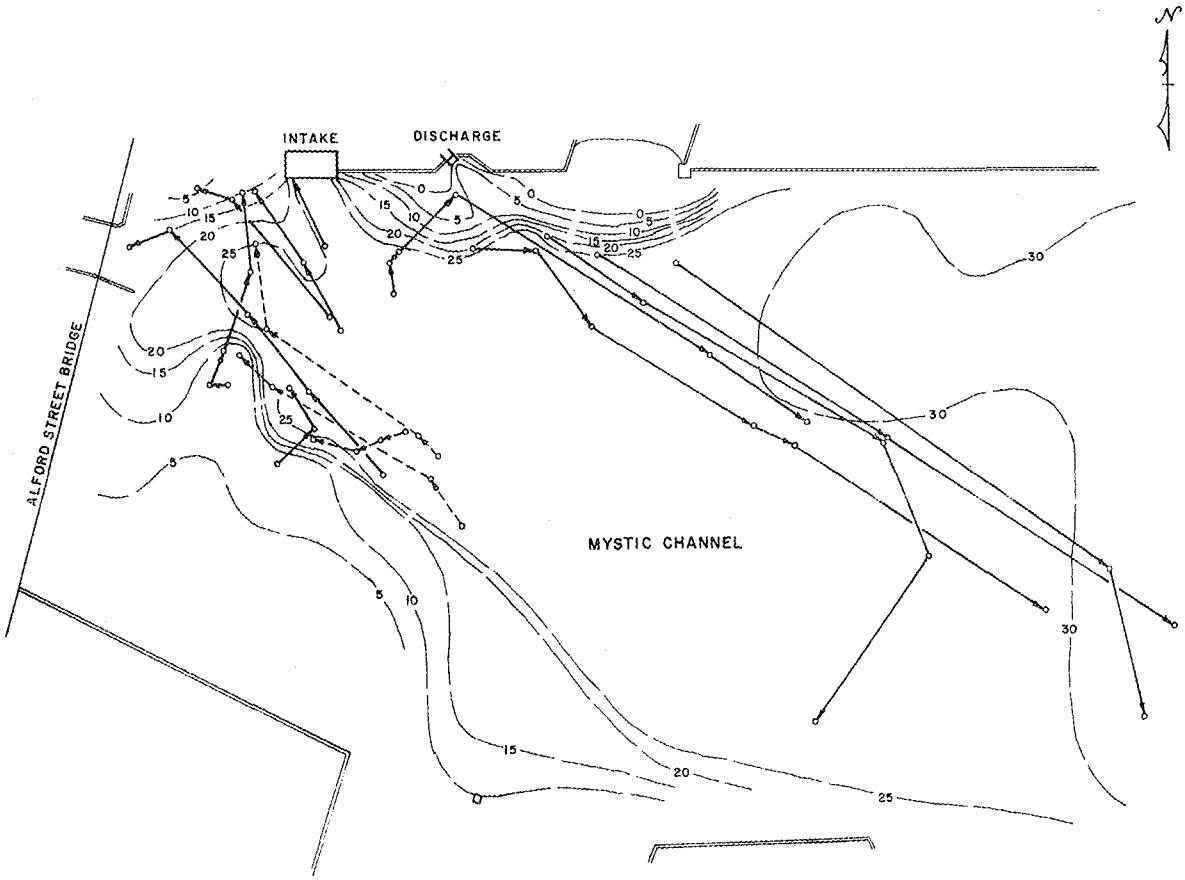

LEGEND:

- o TRIANGULATED POSITION OF DROGUE
- ---→ L=20 FEET (LOWER LAYER)
- ——→ L=5 FEET (UPPER LAYER)

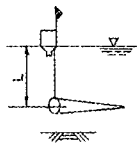

DROGUE DETAIL

NOTES:

1. STAGE: 8' TO 1' SEPTEMBER 17, 1970.
2. DEPTH CONTOURS ARE FEET BELOW MEAN LOW WATER DATUM SUBTRACT 0.78 FEET FROM DEPTHS TO CONVERT TO BOSTON CITY BASE.

FIG. C-12

CURRENT PATTERN DURING EBB TIDE

MYSTIC STATION
BOSTON EDISON COMPANY

The expression of temperatures in terms of increases above ambient is dependent on the definition of ambient temperature. A temperature rise implies comparison of present conditions at a particular point to those existing naturally, i.e., prior to plant operation. The temperature pattern that would have existed in the Mystic channel prior to plant operation would be very complex and time dependent, due to the natural solar induced stratification of the water at various times of the year and the varying tidal flow. It seems evident that it is impossible to compare present surface temperatures in the discharge plume with natural surface temperatures prior to plant operation. Therefore, the plume temperatures are compared to the lower colder water flowing upstream into the Mystic channel at the location of the Tobin Bridge. This section was chosen since water farther out in Boston Harbor is affected by other heat sources, and since water farther upstream in the Mystic channel may be affected by the plant discharge. Analysis of data presented below indicates the ambient bottom temperature was 60 F. It should be recognized that using this ambient temperature results in higher temperature rises than would be the case if a "natural" surface ambient temperature were used.

Figure C-13 shows the surface temperature rise along the plume during various intervals of the tidal cycle, based on the above described definition of ambient temperature. As previously

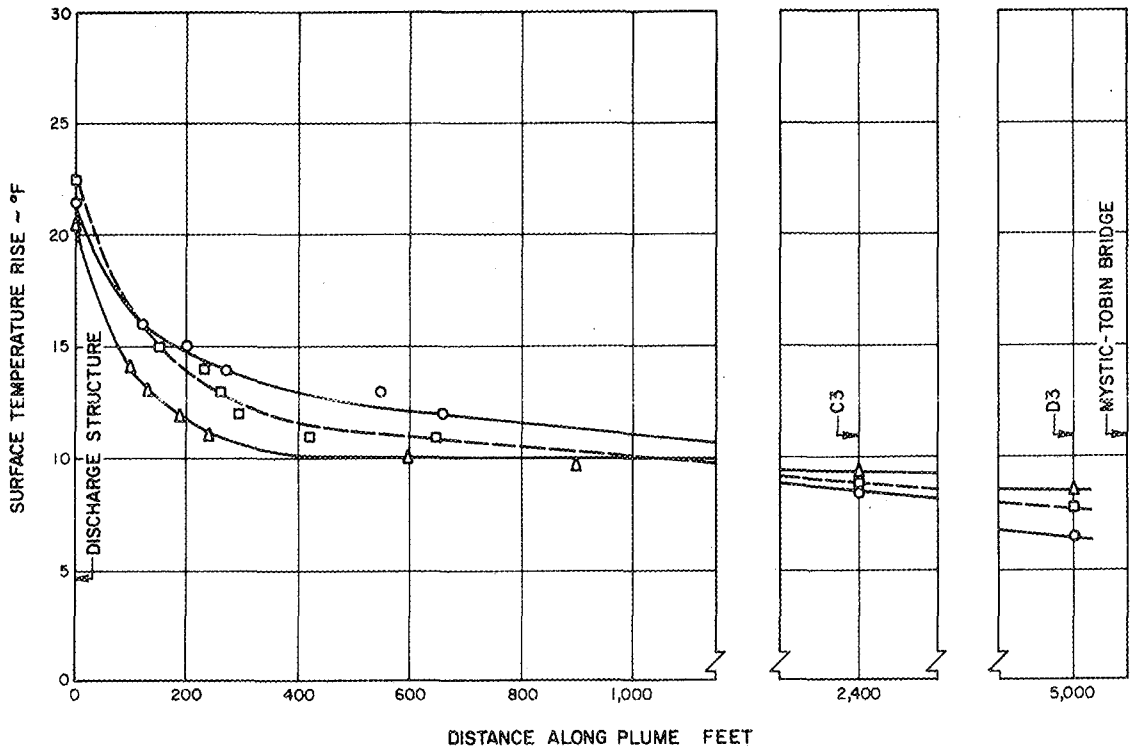

LEGEND:

—○— FLOOD TIDE
—△— HIGH TIDE
—□— EBB TIDE

NOTES:

1. SURFACE TEMPERATURE RISES BASED ON COLDER BOTTOM WATER AT MYSTIC-TOBIN BRIDGE.
2. AMBIENT = 60° F

FIG. C-13
DECAY OF SURFACE TEMPERATURE RISE VS. DISTANCE FROM PLANT
MYSTIC STATION
BOSTON EDISON COMPANY

described, the plume has the lowest temperature rise during high tide and the greatest temperature rise during maximum flood tide. At station D3, 5,000 feet from the plant discharge and just upstream from the Tobin Bridge, the temperature rise varied from 6.4 to 8.5 F. Those temperature rises would be lower if a natural surface temperature could be defined as ambient.

e. Thermal Structure in Mystic Channel

Figure C-14 illustrates temperature profiles versus time in front of the plant intake, and at locations A3, B2 and D3. The locations of these stations are shown in Figure C-1. The lines of constant temperature of Figure C-14, termed isotherms, indicate how the two layer thermal structure varies with the tide both upstream and downstream from the plant discharge.

The data at the intake and at A3, both upstream from the plant discharge, show that the isotherms are more uniformly spaced with depth during the flood tide. This indicates some mixing of the warmer surface water with the colder lower water. During high and ebb tide, the warmer isotherms are more closely spaced nearer the surface, indicating a more distinct two-layer system. Data for locations B2 and D3, both downstream from the plant discharge, indicate that the warmer isotherms remain nearer the surface throughout the tidal cycle. These trends were previously

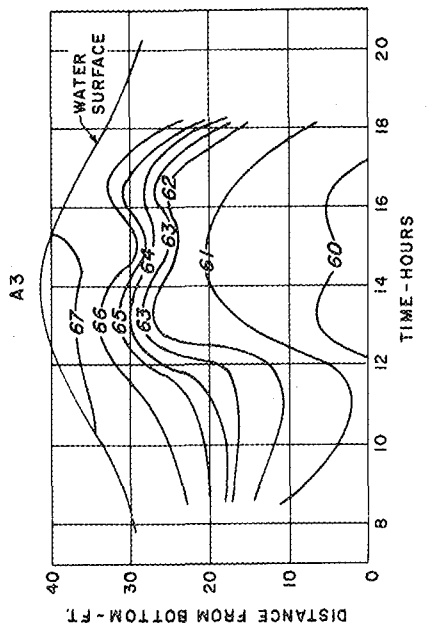

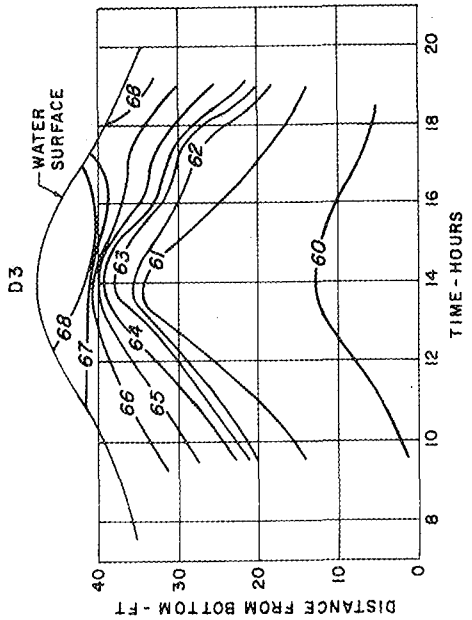

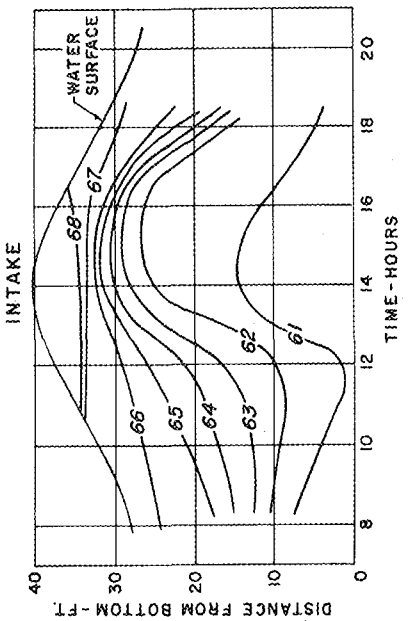

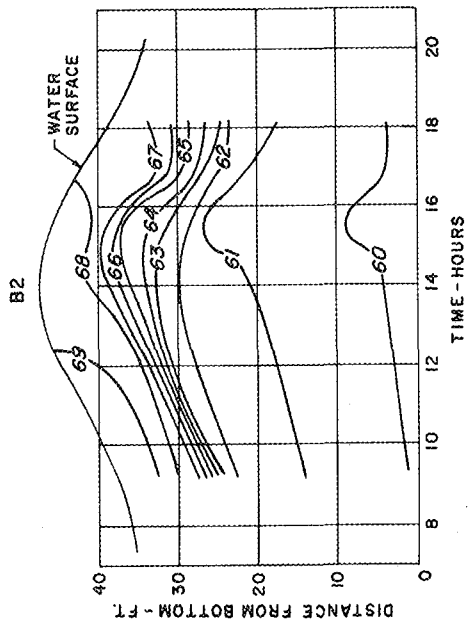

FIG. C-14

TEMPERATURE STRUCTURE DURING TIDAL CYCLE

MYSTIC STATION

BOSTON EDISON COMPANY

mentioned with respect to the temperature profiles shown in Figures C-7, C-9 and C-11.

Data from Station D3, Figure C-14, illustrates the choice of ambient temperature used to compute the surface temperature rises of Figure C-13. As shown, the colder bottom layer remains at essentially 60 F throughout the entire tidal cycle. This lower layer water continually flows upstream from the inner harbor to the plant, due to operation of the circulating water pumps and entrainment into the discharge plume.

The relationship between temperatures along transect D-D and temperatures elsewhere in the inner harbor is shown in Figure C-15. This figure illustrates the cooling of the surface water in the inner harbor and the gradual increase in temperature of the bottom layer flowing into the harbor and upstream into the Mystic channel.

E. Dye Recirculation

A summary of the data collected during the dye recirculation study is presented in Figure C-16. The figure shows:

a. Temperature profiles in front of the intake structure vs. time

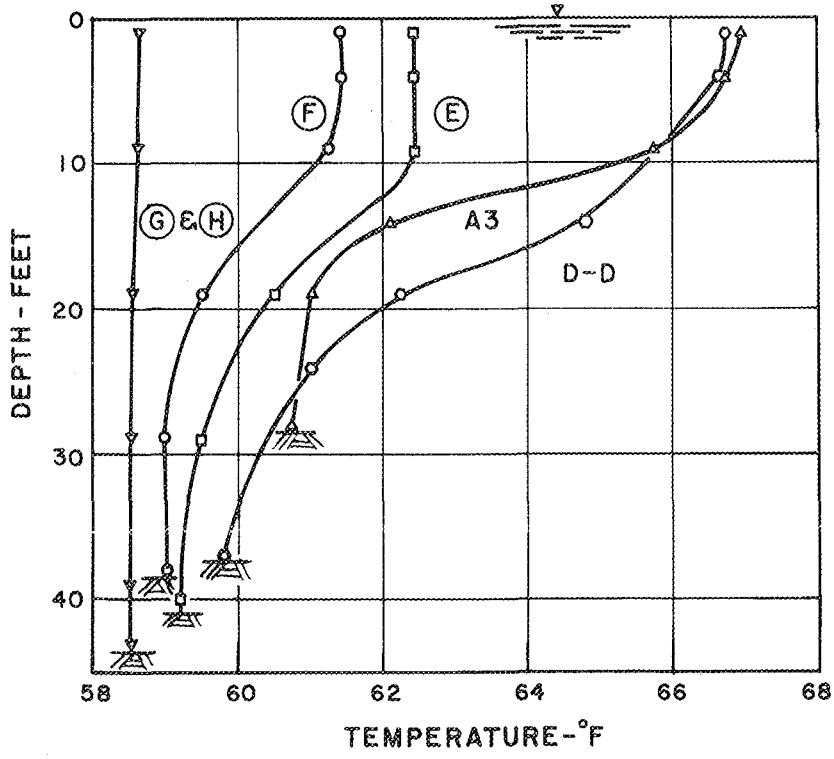

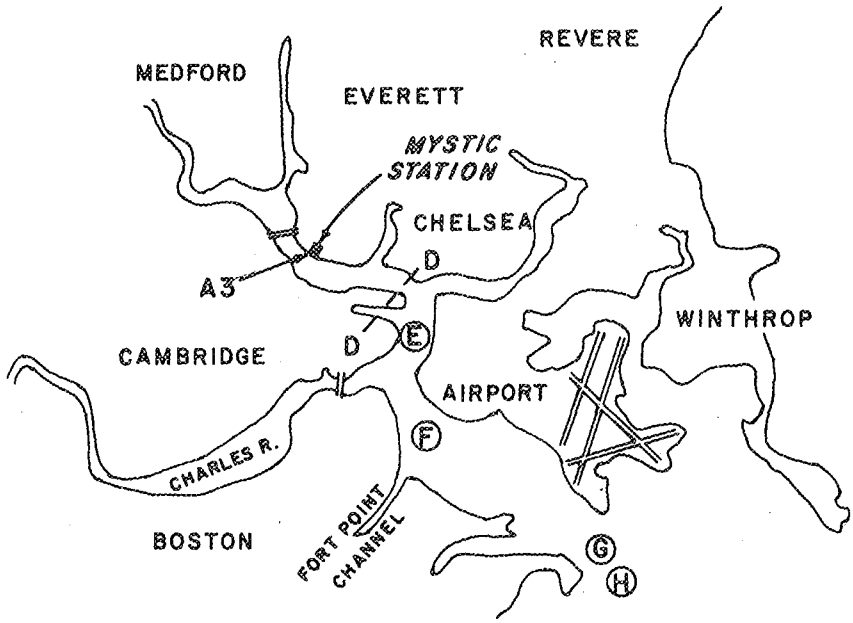

NOTES:

1. ALL PROFILES TAKEN BETWEEN 8:30 AND 10:30 A M, FLOOD TIDE, SEPTEMBER 18, 1970.
2. PROFILES A3, E, F, G & H ARE AT A SINGLE LOCATION.
3. D-D IS AN AVERAGE OF DATA RECORDED AT 5 POINTS.

FIG. C-15

TEMPERATURE PROFILES ALONG INNER HARBOR

MYSTIC STATION

BOSTON EDISON COMPANY

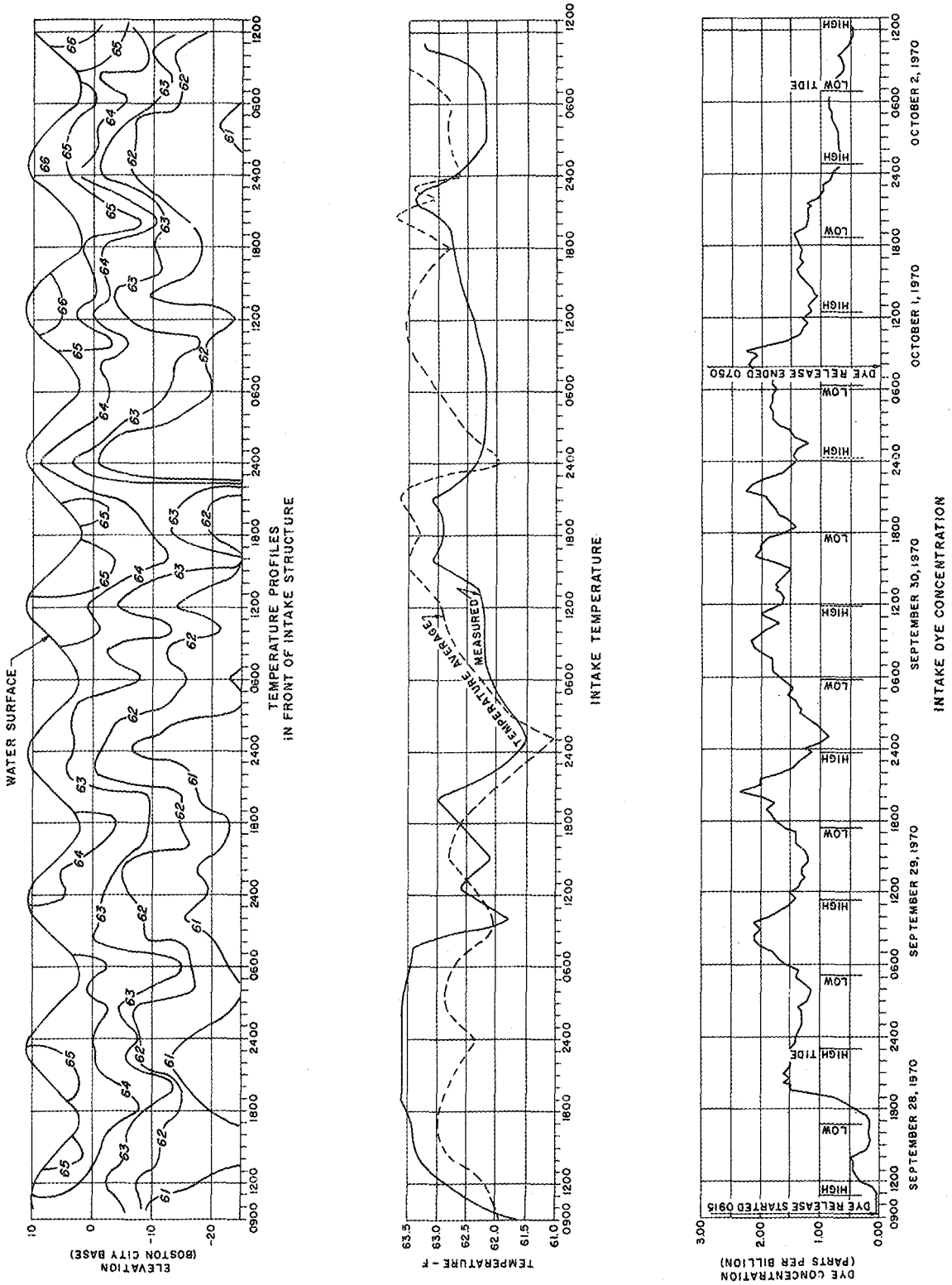

FIG. C-16

INTAKE DYE CONCENTRATIONS AND TEMPERATURES

SEPTEMBER 28 - OCTOBER 2, 1970

MYSTIC STATION

BOSTON EDISON COMPANY

b. Intake temperature downstream of a screen wash pump vs. time

c. Intake dye concentration vs. time

The intake concentration record shows initial sensing of dye within 2 hours after the start of dye injection. Less than 24 hours later, a steady-state condition was reached such that the intake dye concentration repeated in a cyclical manner with the tide.

After dye injection was stopped, the intake dye concentration began to fall. Combined with the fact that dye was sensed in the intake a few hours after the start of dye injection, this indicated that the dye measured in the intake was due to recirculation from the plant discharge and not due to another source.

In general, the peak concentration occurred during maximum flood tide and minimum concentration during maximum ebb tide. This is consistent with the current and temperature survey which showed some mixing of the discharged water with the lower water in a large clockwise eddy during maximum flood tide.

The percentage recirculation is determined from the ratio of the intake dye concentration to the discharge concentration. The discharge concentration is the sum of the dye concentration, produced in the discharge canal by injection from the chemical proportioning pumps and the concentration of the intake water. Therefore, both the intake and discharge concentrations vary, and the most meaningful percentage recirculation is determined from the average intake concentrations as compared to the average discharge concentration. From Figure C-16 it is seen that the average intake concentration is 1.7 parts per billion as compared to the average computed discharge concentration of 9.0 + 1.7 = 10.7 ppb. The average recirculation based on these concentrations is, therefore, 16 percent. The range of maximum to minimum recirculation is only a few percent.

Grab samples of the plant discharge, however, showed an actual average concentration of 12.5 ppb. This indicates that the average plant flow was less than shown by the pump curves. Using this discharge concentration of 12.5 ppb and the average intake concentration of 1.7 ppb results in an average recirculation of approximately 14 percent.

Thus, the average recirculation was taken to be between 14 percent and 16 percent.

The temperature profiles versus time in front of the intake show that, in general, the lower colder layer occupies a greater depth near high tide as compared to other portions of the tidal cycle. To determine the effectiveness of the present curtain wall at the intake, shown in Figure C-2, the average temperature from the profile data was compared to the intake temperature measured downstream from the screenwash pump. If the intake temperature were significantly lower than the average profile temperature, or equal to the temperature of the lower water layer, selective withdrawal from the lower colder layer would be occurring.

A comparison of the intake data of Figure C-16 with the plant data on Figure C-4 shows that the intake temperatures measured in the tank during the dye study are somewhat higher than the temperature recorded at the pump suction lines for Units 4 and 5 by the plant recorder. This increase in temperature may be due to the flow passing through the high head screenwash pumps prior to reaching the measuring point in the tank. Figure C-16 indicates that this temperature rise must be at least 0.5 F since it is impossible for the actual temperature to be higher than the average of the temperature profile. Assuming that the plant intake temperature is approximately 0.5 F lower than indicated in Figure C-16, it is concluded that the curtain wall may reduce the intake temperature up to approximately 1 F compared to conditions without the curtain wall.

VI. SUMMARY AND CONCLUSIONS

A comprehensive field survey program was conducted to measure temperatures and currents presently in the Mystic channel, particularly in the vicinity of Mystic Station. This survey also included determining bottom topography, a dye study to measure recirculation of plant discharge water to the intake, plant operating data, and meteorological conditions.

The objective of this survey was to provide a thorough understanding of present hydrothermal conditions so that the optimum concept for the intake and discharge of the proposed unit can be developed and predictions of its thermal effects can be made.

Temperature measurements were made by precision thermisters from boats in the plant discharge plume and at various stations in the Mystic channel and inner harbor. Current patterns in the Mystic channel were determined by tracking drogues using triangulation. Bottom topography was measured by a combination of fathometry and depth soundings. Recirculation was determined by injecting small amounts of fluorescent dye into the plant discharge and continuously monitoring the intake water with a fluorometer for five days. All measurements were made with the plant operating near 500 MW and over at least one complete tidal cycle.

The dye recirculation study showed that, on the average, 14 to 16 percent of the flow discharged from the plant was pulled back into the intake structure. A continuous plot of intake dye concentration versus time showed that the concentration peaked during the maximum flood tide and was a minimum during the maximum ebb tide. The large clockwise eddy and mixing of the warmer surface discharge water with the lower layer during maximum flood tide probably produced the concentration peak at that time. The data showed that a steady-state condition was reached and that the range of average peak to average minimum recirculation was only a few percent.

Plume temperatures and current patterns from this survey were plotted for periods near maximum flood, high and maximum ebb portions of the tide cycle. This data indicates that plume temperatures are lowest during high tide, highest during maximum flood tide, and intermediate during maximum ebb tide. The lower temperatures during high tide are due to the higher water level which mitigates the restricting effects of a shallow bottom area near the discharge structure and due to lower plant discharge temperatures. Using the colder lower layer water at the Mystic-Tobin Bridge as ambient, the temperature rise of the warmer surface waters at this location varies from 6.4 to 8.5 F.

Flow patterns during these tidal portions show that a large clockwise eddy exists in the Mystic channel opposite the plant, and carries some of the warmer discharged water upstream. Temperature profiles indicate that during maximum flood tide, some of the warmer surface water is mixed with the lower colder water as the flow moves upstream in the eddy.

Both temperature data and observed flow patterns showed the existence of a two-layer flow system throughout the Mystic channel. This flow system consisted of the warmer plant discharge flowing outward over a colder incoming bottom layer of water. Temperature profiles in Boston Harbor indicated that the lower layer is pulled upstream from the harbor entrance to the Mystic Station. The driving force for this upstream flow is primarily produced by the plant circulating water pumps and by the dilution mechanism of the discharge plume. Natural tidal flows at the plant are relatively small since the Amelia Earhart Lock and Dam blocks the Mystic channel just upstream from the plant. Observed flow patterns showed that the upstream flow of colder bottom water persisted during all portions of the tidal cycle.

VII. ACKNOWLEDGMENTS

Stone & Webster Engineering Corporation prepared the scope of the field study and coordinated all phases to and during the survey. Boston Edison Company supplied the plant operating data. Environmental Equipment Division of E.G.& G. International, Waltham, Massachusetts, conducted the survey and was responsible for subcontracting the surveying and dye tracer portions of the study. Gale Engineering Company, Braintree, Massachusetts, surveyed the drogue positions, and Aquatec Inc., South Burlington, Vermont, conducted the dye tracer measurements. Evaluation and graphical summary of the field data was by Stone & Webster Engineering Corporation.

1. Introduction

Predictions of the effects of condenser cooling water discharge on Mystic River water temperatures were based on a comprehensive hydrothermal analysis. The method of analysis can be described by the following steps: field hydrothermal survey, feasibility analysis, and numerical predictions.

The field survey was conducted to study the existing flow characteristics and the thermal structure of the Mystic Channel. Analysis was then continued to investigate the effects of the addition of the seventh unit on the present flow characteristics. With an understanding of the mechanics of the physical system, appropriate mathematical formulations were employed for numerical predictions. This appendix will detail the above procedure and present the major steps involved in the analysis.

2. Field Survey Recapitulation

A detailed description of the 1970 field survey is presented in Appendix C. This section will only discuss some of the highlights which are directly related to the hydrothermal analysis.

The present six units (Units 1-6) of the Mystic Station require a total flow of 780 cfs for cooling the condensers. The cooling water temperature rise above the intake water is 18 F at full load. During the field survey, the heat recirculation rate was found to be 13 to 15 percent of the total station heat rejection rate.

Based on the tidal prism concept, the average tidal current in the Mystic Channel is estimated to be on the order of 0.1 fps. The movement of the thermal plume, which stayed in the upper layer, was found to be in the downstream direction throughout the tidal cycle. The direction of plume movement does not appear to be affected by the weak tidal current.

From water temperature decay patterns measured during the 1970 field survey, the mechanics of the mixing process in the Mystic Channel can be characterized as a near-field jet entrainment mixing and a far-field two-layer flow system.

Within the first 400 to 500 feet from the discharge outfall, the water temperature reduction is rather rapid as compared to the temperature decay at larger distances. The thermal jet with large initial momentum generates turbulence and produces a high entrainment rate, which causes the temperature reduction rate to be relatively large. The mixing process at this near field is

dominated by the discharge condition and may be characterized by the jet densimetric Froude number.

As the distance away from the outfall increases, the jet momentum gradually decreases as a result of both the boundary and internal frictions. At the same time, the kinetic jet energy is gradually dissipated through the generation of turbulent energy. The density difference between the diluted warm discharge and the relatively cool ambient water will have a relatively greater influence on the flow pattern. A second stage of mixing process is then developed at the far field.

Due to density differences, the warm, lighter water will rise above the cool, heavier water. The differences in water temperature result in a density stratification. The natural turbulence level is suppressed by this density stratification, and the mixing process between the warm and cool waters is reduced. Therefore, the warm surface water temperature reduction is a function only of the limited entrainment of the lower cool water and a slow process of surface heat transfer.

The temperature measurements taken at the far field clearly demonstrated the existence of a two-layer flow system. The stability of this two-layer flow is determined by a densimetric Froude Number, F_h, defined by:

$$F_h = \frac{V_r}{\sqrt{\frac{\Delta P}{\rho_o} gh}}$$

where: V_r = relative velocity between two layers,

$\Delta \rho$ = mean density difference between two layers

ρ_o = density of lower layer,

g = gravitational acceleration, and

h = thickness of the surface layer.

When the value of F_h exceeds 0.75, the flow system is generally considered to be unstable.

As the temperature of the warm water is further reduced such that the two-layer flow becomes unstable, mixing between the two layers will be promoted by the natural turbulence. The temperature gradient will decrease, and an isothermal condition may be expected. This is the case at large distances away from the heat source. It was shown during the survey that mild

stratification existed within the Boston Inner Harbor. At the Outer Harbor, the water temperature was essentially homogeneous.

The results of the field survey demonstrated that two different flow regimes exist in the Mystic Channel. At the near field, the thermal jet dominates the mixing process and at the far field, a two-layer flow system prevails. The warm surface layer moves out of the channel throughout the tidal cycle.

It should be emphasized that the rapid temperature decay experienced in the near field during the entire tide cycle, for a continuous and steady discharge of cooling water, clearly indicated that cold water from the outer harbor was induced toward the intake and discharge area. Since the surface area of the Mystic Channel is too small to dissipate a significant portion of the station-rejected heat, the amount of induced cold bottom flow should be proportional to the station cooling water flow times the dilution rate.

The water level fluctuation along the Mystic Channel is due to the long wave propagation of the astronomical tide. The length of the tidal wave is, in general, several hundred miles. The water level along the Mystic Channel is merely moved up and down horizontally without any noticeable slope by the tidal action.

The momentum and energy of the warm water discharge and the density differences tend to overcome the weak tidal movement.

3. Feasibility Study

Consideration was then given to the effect on the present flow system due to the addition of the seventh unit at Mystic Station. With Unit 7, the total cooling water flow will increase to 1,425 cfs, with a composite temperature rise of 18.9 F at rated load.

In the vicinity of the discharge outfall, turbulent mixing of the buoyant discharge jet with surrounding water will occur. In order to facilitate the access of cool diluting water, local dredging is planned to remove a portion of the bottom shelf near the outfall to El.-25.0 feet.

Since the cooling water is also withdrawn from the Mystic Channel, a portion of the heat discharged from the outfall structure will recirculate into the plant. The result of this recirculation and the reentrainment of diluted warm water into the discharge jet plume will increase the near-field water temperature and cause a temperature buildup. The near-field temperature will increase to the extent that the density difference between upper and lower layer is sufficient to develop

a stratified flow condition. Once this stratified flow is formed, the upper layer which carried the station-rejected heat would move out the channel, and the induced cold bottom layer water would move from Outer Harbor toward the intake area.

It is anticipated that the natural processes, such as the tidal flushing and dispersive mechanisms near the station, cannot dissipate the heat to be rejected. As a consequence, the two-layer flow system will be enhanced to promote the heat dissipation process in the Mystic Channel. The interfacial entrainment will increase the flushing rate as compared to the natural flushing process. The energy for this increase in flushing rate comes from the thermal energy rejected from the power station. The cold water in the lower layer would be drawn from Boston Harbor or, ultimately, from the Atlantic Ocean.

It is impossible for the water within the Mystic Channel to increase in temperature indefinitely. It is also impossible for Mystic Channel to function strictly as a cooling pond because of the open connection with Boston Harbor. Based on the above physical reasoning, the addition of Unit 7 can only strengthen the present two-layer flow system at the far field. The question remaining is to what extent the surface layer temperature will rise for a stable two-layer system.

The stability of the two-layer flow system was examined by the criteria discussed in the previous section with the consideration of the new discharge condition. A relationship between the temperature rise of the surface layer and its thickness was developed for a stable stratified far-field condition. It was found that a stable two-layer flow system can only exist when the surface temperature rise exceeds 6.5 F in the near-field area. In other words, the temperature at the near-field area will build up to approximately 6 or 7 F above ambient.

4. Method of Thermal Prediction

The methods for temperature prediction at the near and far fields are different. The temperature rise above ambient necessary to support two-layer flow was first assumed. The dilution of the thermal jet was calculated step-by-step until the turbulent jet plume could no longer be defined. The length of near field is approximately 80 times the initial equivalent jet diameter.

The far-field temperature computation was then made. The temperature obtained from the last step of near-field predictions served as the initial condition for far-field prediction. Again, the procedure was stepwise. The stability of the two-layer flow was checked for each step to ensure the existence of two layers. When the flow was found to be unstable, a new initial assumption

was made for the near-field ambient temperature rise, and the computation was repeated.

The near-field jet dilution computation was based on the relationship proposed by Jen, Wiegel and Mobarek[1], i.e.,

$$\frac{\Delta T}{\Delta T_o} = \frac{7D_o}{X} \exp\left[-3F_h^{\frac{1}{2}} \left(\frac{Y}{X}\right)^2\right] \qquad (1)$$

where ΔT = temperature difference between warm and ambient water

ΔT_o = initial temperature difference between warm and ambient water at discharge point

D_o = equivalent diameter of a noncircular orifice

X = distance from the discharge point downstream along the jet center line

F_h = densimetric Froude number of the thermal jet

y = horizontal distance as measured normally from the jet center line

It is of interest to note that Equation (1) closely resembles the diffusion of a nonbuoyant momentum jet as reported by Albertson, et al[2]. A separate experimental study conducted by Stolzenbach and Harleman[3] found that Equation (1) is adequate for the near-field area.

The motion of fluid at the far-field area can be assumed to be two-dimensional because of the large length-to-width ratio of the Mystic Channel. The conservation equations governing the fluid motion are:

Continuity

$$\frac{\partial \mu}{\partial x} + \frac{\partial v}{\partial y} = 0 \qquad (2)$$

X-Direction Momentum

$$\mu \frac{\partial \mu}{\partial x} + v \frac{\partial \mu}{\partial y} = - \frac{1}{\rho} \frac{\partial \rho}{\partial x} + \frac{\partial \tau_{xy}}{\partial y} \qquad (3)$$

y-Direction Momentum

$$0 = - \frac{1}{\rho} \frac{\partial \rho}{\partial y} - g \qquad (4)$$

Heat (In Terms of Temperature)

$$\mu \frac{\partial T}{\partial x} + \nu \frac{\partial T}{\partial y} = \frac{\partial}{\partial y}\left(K_y \frac{\partial T}{\partial y}\right) \qquad (5)$$

where x, y = longitudinal and vertical coordinates

p = pressure

τ_{xy} = stress tensor in x-y plane

ρ = density of fluid

T = temperature

μ, ν = velocity components in x and y direction, respectively

It should be noted that a hydrostatic assumption is implicit in Equation (4). It should also be noted that at $y = \eta$, or water surface,

$$K_y \frac{\partial T}{\partial y}\bigg|_{y=\eta} = \frac{\kappa}{\rho C_p}\left(T - T_o\right) \qquad (6)$$

where κ = surface heat exchange coefficient

C_p = specific heat of water

T_e = equilibrium temperature

The development of working equations involves integration of the conservation equations over the regions of upper and lower layers. Each layer was treated as vertically homogeneous. Discontinuities in velocity and fluid properties were observed mathematically along the interface. Leibnitz's rule (4) and the kinetic surface condition,

$$\frac{D\eta}{D\tau} = 0 \tag{7}$$

are extensively applied during the integration.

Integration on Equations (2) to (5) yields

$$\frac{\partial[\mu_1 h_1]}{\partial x} = \omega \tag{8}$$

$$\frac{\partial[\mu_2 h_2]}{\partial x} = -\omega \tag{9}$$

$$\frac{\partial[\mu_1^2 h_1]}{\partial x} = \frac{h_1}{2}\frac{\partial g'}{\partial x} - h_1 g \frac{\partial \eta}{\partial x} - \frac{f_i}{8}[\mu_1 - \mu_2]^2 \qquad (10)$$

$$\frac{\partial[\mu_2^2 h_2]}{\partial x} = h_1 h_2 \frac{\partial g'}{\partial x} + h_2 g' \frac{\partial h_1}{\partial x} - g h_2 \frac{\partial \eta}{\partial x} + \frac{f_i}{8}[\mu_1 - \mu_2]^2 + \frac{f_o}{8}\mu_2^2 \qquad (11)$$

and

$$\frac{\partial}{\partial x}\left(\Delta T_1 \mu_1 h_1\right) = -\frac{\kappa}{\rho_o C_p}\Delta T_1 \qquad (12)$$

where h = thickness of the layer

$\underline{w}$ = entrainment velocity

g' = $(\Delta \rho / \rho_o)\, g$

fi = friction factor along the interface

fo = friction factor for the channel bottom

ΔT_1 = excess temperature above the natural ambient water

The subscripts 1 and 2 refer to the surface and bottom layers, respectively.

According to Lean and Whillock[5], the entrainment velocity, W, is defined as

$$W = 0.0025\ (U_1 - U_2)F_h^4 \qquad (13)$$

where F_h is the same as defined earlier.

Since ΔT_1 and ΔP are related, Equations (8) and (12) can be solved simultaneously with known boundary conditions at the beginning of the far field.

As discussed in Section 2, the tidal current is very weak in the Mystic Channel, and the tide is a long-wave phenomenon with a wave length much longer than the length of the Channel. Therefore, the effect of tide on the two-layer flow need be considered only on the depth of water in the Channel.

Approximate solutions can be obtained by further simplification on Equation (10).

$$\frac{\partial[\mu_1^2 h_1]}{\partial x} = 0 \qquad (14)$$

with

$$h_1 + h_2 = H \tag{15}$$

where H = total water depth of the channel.

By doing so, solutions on U_3, U_2, h_1, h_2, T_2 can be determined by Equations (8), (9), (12), (14), and (15).

Numerical computation proceeded by a finite increment ΔX. At each increment, the densimetric Froude number was determined to check the stability of the two-layer flow system.

REFERENCES

1. Jon, Y., Wiegel, R.L., and Mobarek, I., "Surface Discharge of Horizontal Warm-Water Jets," Journal of the Power Division, ASCE, Vol. 92, No. PO2, April, 1966

2. Albertson, J.M., Dai, Y.B., Jensen, R.A., and Rouse, H., "Diffusion of Submerged Jets," Transactions, ASCE, Vol. 115, 1950.

3. Stolzenbach, K.D., and Harleman, D.R.F., "An Analytical and Experimental Investigation of Surface Discharges of Heated Water," Water Pollution Control Research Series, 16130 DJU 02/71, Environmental Protection Agency, February, 1971.

4. Hildebrand, F.B., Advanced Calculus for Applications, Prentice-Hall Inc., 1962.

5. Lean, G.H., and Whillock, A.Z., "The Behavior of a Warm Water Layer Flow over Still Water," 11th International Conference, IAHR, Lenigrad, Paper 2.9, 1965.